

# Mechanical Motion Rectifier Based Single and Hybrid Input Marine Energy Harvester Analysis, Design and Basin Test Validation

Shuo Chen

Thesis submitted to the Faculty of the  
Virginia Polytechnic Institute and State University  
in partial fulfillment of the requirements for the degree of

Master of Science  
in  
Mechanical Engineering

Lei Zuo, Chair

Yaling Yang

Danesh Tafti

February 25th 2021

Blacksburg, Virginia

Keywords: Marine Energy Harvester – Mechanical Motion Rectifier – Power Take-off –

Wave Energy Converter – Hybrid System - HWCEC

Copyright 2021, Shuo Chen

# Mechanical Motion Rectifier Based Single and Hybrid Input Marine Energy Harvester Analysis, Design and Basin Test Validation

Shuo Chen

(ABSTRACT)

Point absorber style marine energy harvesters have been investigated based on their structure, energy harvesting efficiency, and reliability along with costs. However, due to the continuously varying ocean conditions and climates, the system usually suffers low power output and reliability from low input and high Peak to Average Ratio (PAR). Therefore, a Mechanical Motion Rectifier (MMR) based point absorber is introduced in this thesis to promote the harvesting efficiency and reduce the PAR by unifying the input rotation, and allow disengagement inside the gearbox during low power output phase. A 1:20 scale full system was then designed, prototyped, and tested based on the MMR. The bench test results show that the proposed MMR based point absorber could improve the energy conversion efficiency by 10 percent, which brings feasibility to the implementation.

Traditional Wave Energy Converter(WEC) can only harvest ocean waves while ocean current is also one of the significant energy sources widely existing in ocean. In order to further increase the energy harvesting efficiency, one individual energy input source shows its limits. A vast majority of places around the world tends to co-exist both marine waves and current, and extracting energy from both sources could potentially increase the electric power output. Therefore, the Hybrid Wave and Current Energy Harvester (HWCEC) is introduced along with the hybrid gearbox. It is capable of harvesting energy from both ocean waves and current simultaneously so that the electric power output is significantly higher from a combined system. Tank test data shows 38-79 percent of electric power output promotion

of an HWCEC compared to a regular WEC, and 70 percent reduced PAR in irregular wave condition. After that, system electric damping has been thoroughly investigated on both electrical side and mechanical side. The best power output corresponding electrical resistance is identical to the generator internal resistance while the best gear ratio of 3.5 is determined via both simulation and tank test. Furthermore, the system's PAR has been investigated by analyzing the trend of the peak occurrence. Tank test data shows the HWCEC's output power peak occurrence is at roughly 20 percent located at its PAR average. Therefore, the HWCEC system can promote energy harvesting efficiency to the combined system design, and improve its reliability from a significantly reduced peak to average ratio. It also gives HWCEC a large variety of deployable locations compared to a regular WEC under more marine environment.

Furthermore, a new design of the Hybrid model, Hybrid LITE, is then developed, which not only features the HWCEC features, but also a lightweight, immersive and inflatable design for fast deployment and transportation. Since the system is built with an open water chassis, the overall system robustness is significantly improved since no water sealing is required on the powertrain compared to the HWCEC.

# Mechanical Motion Rectifier Based Single and Hybrid Input Marine Energy Harvester Analysis, Design and Basin Test Validation

Shuo Chen

(GENERAL AUDIENCE ABSTRACT)

Ocean contains enormous amount of Marine Hydrokinetic (MHK) energy including ocean waves, tidal streams, and ocean current. Marine energy was investigated due to its continuous, massive and high-density hydrokinetic power output. In order to better serve the needs for ocean surface applications and take advantage of high energy density compared to other renewable energy sources, Wave Energy Converters (WEC) has been investigated, which harvests energy from the ocean wave. In the past years of study, it came to our attention that places such as the west coast of the U.S., northern Europe, and the Mediterranean area tend to have both abundant marine wave and current energy. Therefore, a new design of the Hybrid Wave and Current Energy Converter (HWCEC) is investigated for higher power output. In order to combine the energy sources from waves and current, a Hybrid Gearbox was selected to joint the power and unifies the motion from the wave for a higher efficiency. Simulations and 1:10 ratio co-existing wave and current basin test have been conducted for the HWCEC. By using the same system, single wave or current input are used as the baselines and the dual input HWCEC has demonstrated great benefit and potential. The electric damping and the gearbox ratio of the HWCEC are studied for the best power output in both simulation and tank test. The result shows that the HWCEC could promote up to 38-71 percent of electricity output in a regular wave condition, and 79 percent in irregular wave condition. The Peak to Average Ratio (PAR) is a key factor for system's mechanical reliability. The testing shows that the HWCEC can reduce 70 percent of the peak motion

and contribute to the average, which is an indirect indicator of the system's better reliability. Furthermore, to align the needs of the design for real life applications, The Hybrid LITE Converter idea was then developed for special deployment requirements for the future application of the Hybrid system. It has a novel open-system design with the implementation of a newly designed hybrid gearbox. This converter has the potential of promoting reliability, deployability and weight reduction for easy transportation from its open system design compared to HWCEC. The system modeling could be done as future work varies from the changing deployment locations for higher electric power output.

# Dedication

*I dedicate my work to Prof. Lei Zuo for his support, kindness, and guidance in my academic studies and my life. He has shown great patients and effort in teaching me mechanical designs and calculations. He has inspired me to look deeper into design works and oftentimes, sparkles of ideas light up the palace of solutions. Four years in and he can still surprise me with his ideas and mindset.*

*I also dedicate my work to my parents, Prof. Jianming Yang and Dr. Ruofei Chen, who have always been there when I was reaching for the stars and chasing my dreams. This journey can be tough, but with their unconditional care and love, everything seems achievable. When looking in their eyes, I see the purest love I can find on Earth.*

*I would also dedicate my work to Yijia Cen, who has always been there when life became twisted. Her sweetness can always dissolve the bitterness in the past 7 years of being together. Many love and many thanks.*

*Special thanks to my friends, Boxi Jiang, Dr. Xiaofan Li, and Yuzhe Chen for all the help during the study. All of you have been my best cheerleaders with the endless help on the paper publications, engineering designs, and tank tests.*

# Acknowledgments

I wish to thank my committee chair, Dr. Lei Zuo for his countless hours of reflecting, reading, and encouraging in the past years. Many thanks to Prof. Yaling Yang for the help on the competitions and proposals. Her work in wireless communications truly inspired me to look into more possibilities of the ocean energy industry. I would also like to thank Prof. Danesh Tafti for his guidance on the CFD analysis and motivate me to look into more hydrodynamics analysis of the marine energy harvesters.

I also would like to thank Davidson Lab in Stevens Institute of Technology, New Jersey, and Océanide, La Seyne-Sur-Mer, France for supporting our experiments day and night.

Special thanks were given to Boxi Jiang, Dr. Qiaofeng Li, and Xiaofan Li for the help in the data analysis for multiple projects, and this work cannot be accomplished without their dedication. Many thanks to Weihang Lin, Duncan Lambert, Xian Wu, Kan Sun, Qiuchi Xiong, Jia Mi, Dr. Feng Qian, and Dr. Mingyi Liu for the help on the endless projects and smart ideas in the group meetings. Last but not least, many appreciations to Jianuo Huang, who truly dedicated himself to the harvester design work.

I would like to acknowledge the financial support from the United States Department of Energy grant No. DE-EE0007174, DE-NE0008591, European Union Horizon 2020 Framework Program No. 731084, MaRINET2 program. I would also like to acknowledge the funding support from U.S. Environmental Protection Agency grant No. 83991001-0 for the continuous support for the projects.

# Contents

List of Figures	xi
List of Tables	xvi
<b>1 Introduction</b>	<b>1</b>
1.1 Marine Energy . . . . .	1
1.2 Review on Marine Energy Harvesters . . . . .	3
1.3 Challenges and Restrictions . . . . .	6
1.4 Hydrokinetic Wave Energy Harvesters . . . . .	8
1.5 Thesis Organization . . . . .	9
<b>2 Mechanical Motion Rectifier Based WEC</b>	<b>11</b>
2.1 Chapter Introduction . . . . .	11
2.2 Design of the two body WEC with MMR . . . . .	12
2.2.1 MMR Design and Power Transmission . . . . .	15
2.2.2 Analysis on the MMR Dynamics . . . . .	17
2.2.3 PTO Bench Test . . . . .	19
<b>3 Hybrid Energy Converter</b>	<b>22</b>

3.1	HWCEC Introduction . . . . .	22
3.2	Converter Design . . . . .	24
3.2.1	Overall System Design . . . . .	24
3.2.2	Key Component Design . . . . .	26
3.3	Dynamic Modeling . . . . .	32
3.3.1	Two-body WEC baseline . . . . .	33
3.3.2	Turbine Baseline . . . . .	33
3.3.3	Power Take-off . . . . .	34
3.3.4	HWCEC Simulation Results . . . . .	35
<b>4</b>	<b>Basin Test and Discussion</b>	<b>40</b>
4.1	Basin Test . . . . .	40
4.1.1	System Preparation . . . . .	41
4.1.2	Mooring System Layout . . . . .	45
4.1.3	Sensors Selection and Installation . . . . .	47
4.2	Results and Discussion . . . . .	48
4.2.1	Turbine Baseline Test . . . . .	49
4.2.2	WEC Baseline Test . . . . .	50
4.2.3	HWCEC System Performance . . . . .	51
4.3	HWCEC Basin Test Conclusion . . . . .	57

<b>5</b>	<b>Future Work on the Hybrid System</b>	<b>58</b>
5.1	Hybrid LITE System Design . . . . .	58
5.1.1	Hybrid LITE PTO Design . . . . .	58
5.1.2	Hybrid LITE Gearbox Design . . . . .	62
5.2	Future Work Summary . . . . .	66
<b>6</b>	<b>Conclusion</b>	<b>67</b>
	<b>Bibliography</b>	<b>69</b>

# List of Figures

1.1	The figure displays the reference projects published by the Department of Energy.[1] . . . . .	4
1.2	The figures display the iterations of Mechanical Motion Rectifier Gearbox from rack-pinion based rectifier to bevel gears and one-way clutches based rectifier. With the iterations of the gearbox, the system becomes more compact, robust and more efficient. [2] [3] . . . . .	5
2.1	500W MMR based full system design . . . . .	12
2.2	It shows the 1:20 scale 500W system hardware and CAD design. The system is MMR-based, which could help increase the overall efficiency of electric power generation. The tank is composed of two steel cones on each side of the plastic tank, and the two steel cones are connected by the aluminum round bars that are 1-inch in diameter. The final systematic testing has not yet been completed.	15
2.3	Mechanical Motion Rectifier design and power transmission figures. It shows both of the engagement modes. . . . .	16
2.4	System's response for MMR and Non-MMR systems. The top figure shows the force on the system during the operation, and the bottom shows the rotational speed of the system with the disengaged at time of 5s, 10s, 15s, etc. [4] . . . . .	18
2.5	The system's force with respect to time under different resistive loads. [4] . . . . .	18

2.6	The system's force with respect to time under different resistive loads.[4]	19
2.7	System's response with and without the MMR	20
2.8	System's response and effieicny with and without the MMR[4].	21
3.1	Overall system design. Figure A, B, and C shows the overall assembly, Power Take-off System, and Hybrid gearbox connection designs. The figure shows the general power flow and the design of the overall system.	24
3.2	Section view of the hybrid gearbox design with a transparent view to display the one-way clutches. This figure shows the detailed component design of the gearbox.	26
3.3	Hybrid gearbox design and designed wave only input power flow for mode 1. The mode is composed with 2 stages by the varying input rotational direction. Hybrid gearbox operation mode 2, current input only condition; Mode 3, wave and current both input engages, mode 4, no engagements	28
3.4	System hardware demonstration. It showed the general assembly of the HWCEC including the buoy, bottom column, ball screw connection, and Hybrid gearbox	29
3.5	Marine Turbine pressure distribution on both front and back. The fluid velocity is 0.5m/s. The working condition is 15 RPM.	34
3.6	Output power for turbine baseline under different electric damping. The ambient flow velocity is 0.5m/s and the wave period is 2.21s	36
3.7	Comparison between WEC and HWCEC under different electric damping. The ambient flow velocity is 0.5m/s and the wave period is 2.21s	36

3.8	Time domain simulation on (a) rotational speed of the shaft under engagement and disengagement condition (b) HWCEC power output compared to WEC and Turbine only condition. . . . .	38
3.9	Effect of planetary gearbox ratio on the Hybrid device with related to the system's electrical damping. 1:3.5 gear ratio reached the peak in given conditions. . . . .	38
3.10	Varying speed input of the HWCEC with the amount of power generated under different electric damping. Wave height:0.096m, Wave period:2.21s. . .	39
4.1	Dimensions, on-site assembly, trial testing. The current state of the system is extended. . . . .	41
4.2	The basic concept of the system deployment for 5 basic steps . . . . .	42
4.3	The overall layout of the testing facility. The Hybrid Energy converter is moored at the center of the tank while the turbine is always facing the current input direction. . . . .	43
4.4	The detailed layout of the mooring constraint on the Converter. Four mooring lines are distributed across the overall system in order to secure its location and prevent large pitching motion from the wave and current. . . . .	46
4.5	Turbine performance under different gearbox conditions with the change of generator dampings. The peak power is produced with the 3.5 magnification gearbox and reached 0.86W at a 0.5m/s current. . . . .	50
4.6	Experiment data recorded for a test under 0.5m/s current speed and 2.21s period regular wave. (a) Displacement of buoy (b)Angular velocity of input shafts and output shaft . . . . .	51

4.7	Comparison on power output and shaft velocity between the Hybrid device and the WEC device working individually under 10 Ohm loads and working environment. . . . .	52
4.8	Comparison of the output power of WEC, 0.5m/s Hybrid and 0.6m/s Hybrid device with regard to the electric damping at the wave period of 2.21s and wave height of 0.096m. . . . .	53
4.9	HWCEC power output with different gearbox configurations at 0.5m/s current speed. The Wave period is 2.21s and wave height is 0.096m. . . . .	54
4.10	Comparison on output power between WEC and the Hybrid device under irregular waves with 3.06s significant wave periods and 0.12m wave height with 0.6m/s of current input speed. . . . .	55
4.11	PAR and its occurrence for both WEC and HWCEC. The WEC device's ratio is more spread out in a decreasing pattern with the maximum at 15 while the HWCEC concentrates at the ratio of 1 with the maximum at 4. . . . .	56
5.1	Overall Hybrid LITE system design . . . . .	59
5.2	Compact design of the Hybrid LITE system to fit the needs of the clients . . . . .	61
5.3	HLG cross-section view from the side. The figure illustrates the detailed design and components inside the HLG. The left figure shows the general structure of the HLG, which is similar to the hybrid gearbox described in the last chapters but with a different orientation. It helps the design in a narrower environment so that the system is more compact. The right two figures show the dowel pin alignment design to simplify the off-plane O-ring groove design. . . . .	62

5.4	The power transmission of the HLG. The turbine input shaft, buoy input shaft, and output shaft are shown in red, blue, and yellow. Two stages of the HLG are shown so that the power transfer direction can be better seen. . . .	64
5.5	Customized Hybrid LITE Gearbox hardware. It is designed for open water applications with high reliability. Gearbox is ready for next phase hardware testing. . . . .	65

# List of Tables

3.1	The power of the system in different wave height in simulation . . . . .	37
4.1	Ocean environment parameters used in basin test . . . . .	49
4.2	Point absorber baseline tests result . . . . .	50

# Chapter 1

## Introduction

### 1.1 Marine Energy

With the development of technologies, energy consumption has increased tremendously in the past few decades. The world's energy usage in 1999 was 9398 Tonnes of Oil Equivalent (Mtoe), compared to the 13576 Million Mtoe in 2017 [5]. The trend of energy consumption from 1990 to 2017 increase by almost 44 percent, and it is predictable that energy consumption will increase further in the future. Traditional fossil fuels resources such as gasoline and coals have played major roles in the power generations in the past centuries. Therefore, with the recognition of potential climate changes due to the excessive usage of fossil fuels, researches have been conducted on renewable energy such as solar, wind, hydro, geothermal and nuclear, while sometimes nuclear considered as nonrenewable as well. According to the Global Energy Statistical Yearbook, 20 percent of the electricity consumption is generated by renewable energy with only 7.3 percent from hydro, which includes riven dam, and river turbines[5]. Most renewable energy is provided from wind, and solar, the portion of ocean energy is very limited.

Solar, wind, and geothermal energy are sometimes limited by the weather, climate, geographical conditions, which brings difficulties in the application regularly. It is found that they also have some ineluctable drawbacks: the limited power generation ability and a relatively long payback period. Even though nuclear energy is already playing an essential role in

world electricity production, due to problems such as proliferation, national security, safety, waste management, it is almost impossible to widely adopt this around the globe as for now. However, tidal energy density is tens to hundreds denser compared to the solar, wind and geothermal [6], and could be much more easily accepted compared to nuclear. These motivated researchers to look into marine energy as one of the most promising renewable energy sources.

There are a total of two main categories of marine energy that have been widely recognized: marine thermal energy and hydrokinetic energy. The marine thermal energy usually comes from the sun or the earth but the power output is usually in the milliwatts to watts range. The power levels are suitable for scientific research purposes but not enough for other more power demanding applications such as observations or utility purposes, which is capable of reaching watts to megawatts level. The International Energy Agency (IEA) report also shows the expectation of ocean energy generation could reach 15 TWh/year in 2030, while we currently remain at 2 TWh/yr with less than 10 percent of growth rate for the past ten years[7]. The large gap between now and 2030 could be filled with well-developed marine hydrokinetic energy harvesters. Even though ocean energy is still at its infancy, but this promising vision reinforce the importance of the future development of the marine energy industry, and help motivate and guide the industry.

The three types of essential Marine and hydrokinetic (MHK) energy are marine waves, currents, and tides, that could provide enormous potential to provide clean, renewable electricity to communities and cities across the US and the world[8]. According to DOE, the total potential for US wave, tidal, and current hydrokinetic resources is estimated to be 3,285 TWh per year, which is 80 percent of the annual electricity produced in the U.S [9]. Furthermore, ocean covers over 71 percent of the earth's surface, which has great coverage throughout the entire globe and provides great accessibility. With more than 50 percent of

the U.S. population living within 50 miles of coastlines, the potential for the U.S. is huge[9]. Hence, wide marine energy based applications commercialization such as ocean observation and navigation, underwater vehicle powering, agriculture, desalination, disaster recovery, and utility-scale powering are achievable goals according to the Powering the Blue Economy report from the Department of Energy (DOE) in 2019[10].

## 1.2 Review on Marine Energy Harvesters

The study of ocean energy started in 1799, when the first patent was applied in France[11]. However, marine research did not bloom until many later days in the oil crisis in the 1970s. Even though the research started a long time ago, due to the low harvesting rate and lack of reliability in the Power Take-off (PTO) system, not many commercialized marine energy harvesters available on the market as of today. A large variety types of harvesters have been identified through research and most of them takes advantage from ocean wave, current, tidal, and thermal. DOE has released a set of six Reference Model Projects (RMPs) that conclude the types of energy harvester that retrieve electric power from the hydrokinetic power. It provides a standard to better categorize the researched harvesters currently.

In fact, tremendous amount of research has been done on both ocean wave and current energy sources to maximize the power output and increase reliability[12][8]. Typical ocean wave harvesters including point absorber style harvester first proposed by Budal and Falnes in 1975 [13]. The development of the point absorber style WEC was then derived into three categories. Over-topping device, takes advantage of and oscillating body and collect water to the reservoir on top and convert the potential energy to electric energy through the turbine [14]. Oscillating water column which harvest energy from the varying air pressure powered turbine inside the air chamber, which floats on the ocean surface. Falcao et al investigated

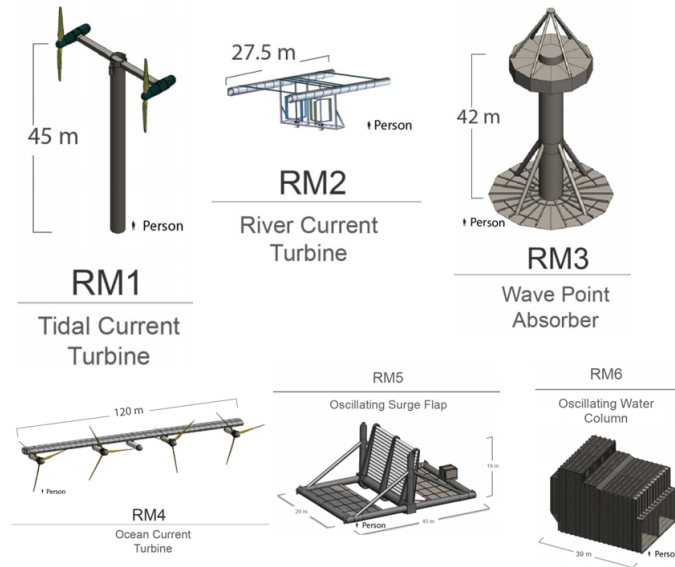


Figure 1.1: The figure displays the reference projects published by the Department of Energy.[1]

in the turbine optimization for higher power output[15][16]. Lastly, the oscillating body converter collects energy from the oscillating wave excitation and power the generator. Typical devices such as SeaBeavl [17] which directly converts the oscillation to electricity by integrating the generator model; French and Bracewell conducted internal mass WEC system design and uses the out of phase motion between the buoy and internal mass to drive generator and collect energy [18]. Other types of WEC including attenuator design, such as Pelamis WEC [19], which is one of the most well-know attenuator design around the world. Pelamis provides a flexible design that is mounted with the direction of the wave propagation, which harvests energy from the relative motion provided by intercepting the ocean wave. Salter's Duck device was invented in 1978, which harvests energy from pitching motion of the nodding to collect energy [20]. On the other hand, ocean current is also abundant and widely available at the same time. Vertical or horizontal current turbine are mostly selected to harvest energy from the running current. Bahaj et al have conducted research on the sizes

and shape optimization of the marine current turbine for maximum energy productions [21]. Dajani et al looked into the marine current turbine angle of attack performance to study the relationship between current speed, direction and angle of attack[22]. Both sources of marine energy in ocean wave and current are playing a significant role in the ocean energy due to their relative abundance and ease of harvesting compared with the other types of marine energy sources.

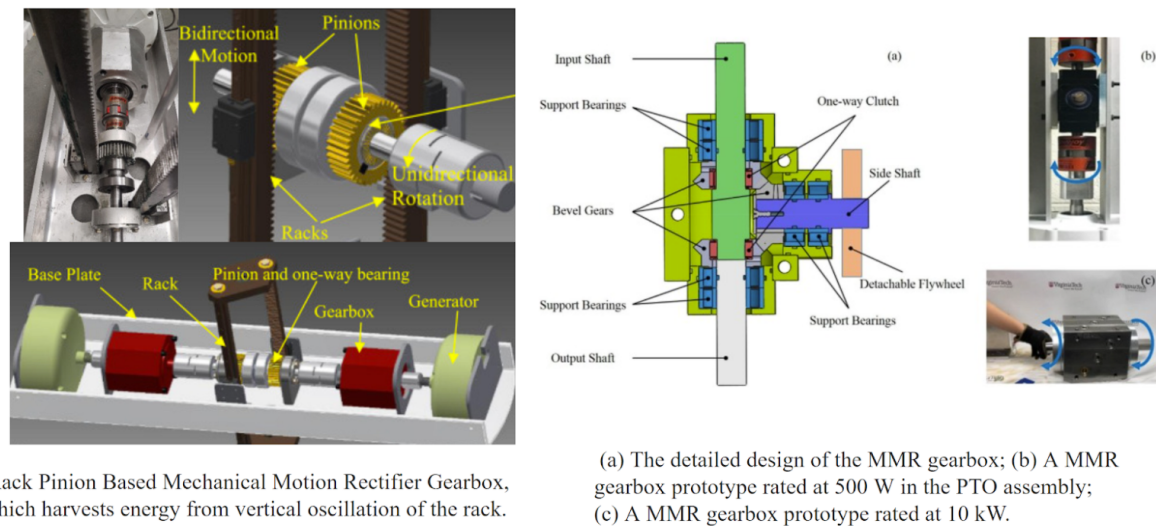


Figure 1.2: The figures display the iterations of Mechanical Motion Rectifier Gearbox from rack-pinion based rectifier to bevel gears and one-way clutches based rectifier. With the iterations of the gearbox, the system becomes more compact, robust and more efficient. [2] [3]

Lots of research has been conducted on a single Reference Model, and researchers expect to create new design methods, best-optimized shape, and most efficient control algorithms to conclude a most efficient prototype with the lowest Levelized Cost of Energy (LCOE). LCOE is the cost of energy production and it is calculated by the lifetime costs divided by energy production. With a lower LCOE value, the system is likely to be more reliable, affordable, and sustainable. However, achieving this goal has always been a challenge for the entire academia and industry [23]. Therefore, researchers have been working on solutions to

reduce the peak to average ratio via mechanical gearboxes. Liang and Zuo has investigated the first generation of a Mechanical Motion Rectifier Gearbox (MMR), which uses a rack and pinion system that converts vertical oscillation into rotational motion for the generator [2]. This design has significantly smooth the power generation curve by reduce the peak power impulse and keep the energy harvesting at a high speed. It also motivated researchers to keep investigating into the MMR based systems for better system performance and robustness.

### 1.3 Challenges and Restrictions

Ocean energy is massive, vast, continuous, and environmentally friendly but yet to be commercialized even with years of work. Challenges appear in cost, reliability and power generation of the marine energy harvesters.

The manufacturing and maintenance cost are usually the most significant investment during the development of the marine energy harvesters. The cost and power output are the significant factors of the LCOE calculations. Sometimes, a high LCOE made it almost an unworthy project to investigate any further. Therefore, the challenges on cost reduction have significantly slowing the speed of the marine energy industry's development.

One of the solution is to increase the reliability of the mechanical system so that the maintenance cost can be reduced. However, while mechanical components continuously operate under a vibrating condition, the structure tends to fail much quicker in real marine conditions. Components such as ball screws, belts and many other mechanical components on the powertrain constantly receive large impact forces from the irregular waves. The failure is almost inevitable from a direct drive system since it's extremely hard to reduce the impulse without losing system efficiency. Therefore, one goal of this thesis is to solve the overall system reliability issue while maintaining or even increasing the system's performance. The

issue appears to be simple but it requests out-of-box thoughts to put together a novel design in order to achieve the goal.

Furthermore, while the system has a higher electric power output, the LCOE tends to go lower even though the cost can not be reduced. However, in a less ideal marine conditions, not much energy can be produced due to the low wave height or current speed, which result in low power output. Therefore, increasing the power output, or energy harvesting efficiency is also a challenge towards the harvesters nowadays.

The three identified factors do not conclude all of the factors of the LCOE calculation, but they are significant factor for the mechanism that is discussed in this thesis. Gearboxes is the main joint of the powertrain of the proposing systems and it is affected heavily by the mentioned factors. Therefore, cost, reliability and power promotion the main topic that this thesis will cover.

The restrictions for the projects can be divided into two larger categories: policies and testing environment. Ocean energy harvesters are mainly mechanical systems that contain lubrication, metals shave, unfastened components, or even sharp edges that could potentially harm the environment or marine creatures. Therefore, all testing under federal fundings requires The National Environmental Policy Act (NEPA) Permit to test in open water unless specified otherwise, which brought challenges to the testing side. The other obstacle is the testing site's regulation, testing period, and facility limitations. Some of the larger-scale energy harvesters are not capable of being tested in a regular civilian used tank since the depth or the width don't meet the requirements of the prototypes. Other devices that require ocean current input as energy source is even more complicated and very few tanks provide that capability. Most labs directly tow the system in the tank to simulate the current input while this solution is instantaneous, which cannot last long limited due to the total length of the tank.

Therefore, all of the challenges and restrictions slows the development and commercialization of the marine energy harvesters due to necessary considerations of the environmental protections. This motivated us to investigate into the details and potentially improve the situation.

## 1.4 Hydrokinetic Wave Energy Harvesters

The wave energy converter (WEC) is a mechanical device that harvests energy from the ocean wave and convert to electricity and point absorber is a very typical WEC device as mentioned. Point absorber contains a buoy that floats on the surface or submerged in the water and oscillate along with the wave. Direct drive mechanism is usually adopted for WEC so that all of the wave input energy can be converted into the point absorber. In this thesis, a point absorber system is typically referred as a WEC system and it is the only types of harvester that this thesis is investigating into with no other types of reference models are being referred to.

Different from a conventional WEC that only harvests wave energy, a hybrid wave and current energy converter (HWCEC) is a mechanical energy harvester that is designed to harvest energy from both marine waves and currents at a higher efficiency since it can combine the two sources and power the generator. Due to the implementation of the turbine, the HWCEC does have a much higher power output and potentially increased reliability due to the low PAR compared to the traditional WEC design.

Furthermore, a special edition of the HWCEC is also designed and it is named Hybrid Wave and Current Energy Converter LITE (Hybrid LITE). This is a novel design based on the HWCEC, which features lightweight, compact, fast deployability, and even lower manufacturing cost. In this design, belt transmission has been adopted and the new concept

of “Open system” is defined. The system is soaked in the water and could operate without frequent maintenance and repair. The sea water will lubricate the system and with no gearbox or generator located submerged in the water, the system is free from rust, leakage, and decomposition.

The WEC system referred in Chapter 2 adopts the traditional MMR design and the HWCEC uses the hybrid gearbox PTO system. The two types of rectifiers are different in the design level and could achieve different goals while not losing their efficiency and reliability. The HWCEC system adopts a Hybrid gearbox that changes the direct drive mechanism, and smooth the operation. With the gearbox’s implementation, the system is operating with a higher efficiency and robustness with less cost in manufacturing and maintenance. The Hybrid LITE device uses a modified hybrid gearbox, which reduces the weight, increases the watertight capabilities and robustness.

Depending on the sizes and designed system rotational speed, both AC and DC generators are selected for different designs to meet the requirements. In general, both types of devices are capable of generating Watts to KiloWatts level of power depending on the scale of the designs.

## **1.5 Thesis Organization**

The following chapters will introduce a MMR based WEC device, simulations and testing results. The system has been fully designed, improved, and assembled for later testing purposes. The in-lab test has been completed and it will be described in chapter 2 to illustrate the benefit of the MMR system compared to a non-mmr WEC device.

Then, the system is targeted to be able to further improved by harvesting two energy sources

simultaneously and it could greatly reduce the cost and even potentially increase the reliability. Therefore, a HWCEC is designed and manufactured to improve the overall operational mechanical efficiency and reliability of the PTO. The HWCEC system prototyping and simulations are explained in the Chapter 3, and the testing results, and discussion will be in Chapter 4.

Chapter 5 introduces the future work to improvement the design of the HWCEC for specific applications, and a HWCEC Lite system is introduced for further PTO improvements. Finally, Chapter 6 concludes all the work in this thesis and list the contribution.

# Chapter 2

## Mechanical Motion Rectifier Based WEC

### 2.1 Chapter Introduction

PTO system design has always been challenging at its low reliability and power output, due to the unpredictable operating environment. This chapter introduces the design and testing of a MMR based WEC rated at 500W. With the implementation of a MMR gearbox, the WEC is able to run more efficiently from the result of testing. With the two unique operational modes of the MMR, the engagement and disengagement mode, the MMR mechanism can significantly promote the gearbox's operational efficiency by disengaging at a low input power while re-engage after the input power matches with the system. Through analysis and lab testing, the advantage of the MMR mechanism is verified, indicating the great potential of a MMR based WEC in real world applications. To give an example, in this chapter, it is combined with a self-reactive two body wave energy converter to demonstrate the working principle and for future testing.

## 2.2 Design of the two body WEC with MMR

The introduced MMR-based Wave Energy Converter is designed to be tested to verify the functionality in the open water, and the prototype's design is rated at 500W. The MMR-based WEC harvests wave energy and transfers the power to electricity by the generator located at the bottom of the PTO column. This system also adopts the MMR mechanism to increase the energy generation efficiency and reduce the peak to average ratio to increase the lifespan of the system.

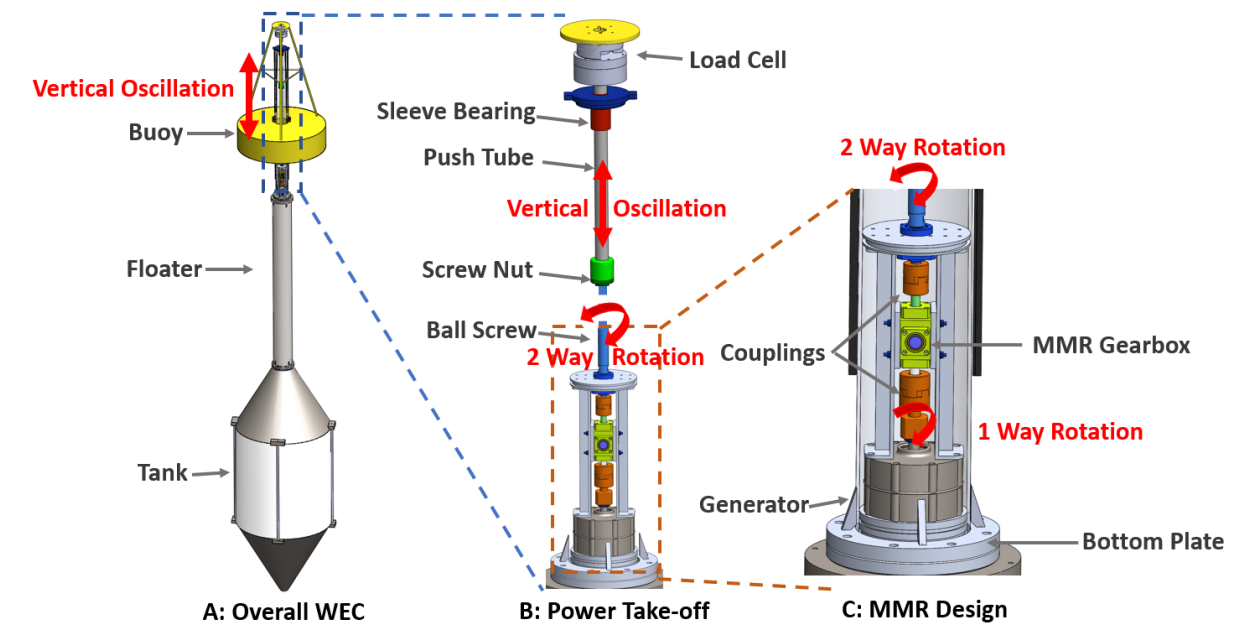


Figure 2.1: 500W MMR based full system design

From the top, the buoy is coupled with the push tube on top, which moves simultaneously with the buoy during operation. While the wave oscillation get in contact with the system buoy, the vertical oscillation passes downward from the buoy, through the sensor to the push Tube, which is bolted to the nut of the ball screw. The push tube's functionality is to push and pull the nut and transmit direct force to the ball screw while allowing the ball screw to slide internally. Since ball screw requires two joint connections, so that one end is bolted

at the bottom supports, and the other one is a glider adaptor that fits onto the ball screw end, and help slide inside the push tube. The back driven ball screw system is capable of converting the vertical oscillation to a 2-way rotation, or bi-directional rotation and send it to the Mechanical Motion Rectifier gearbox.

Since torsion can be destructive towards the overall system, the MMR gearbox setup is backed by two frames to secure the stabilization of the PTO. The reference for the frames is set to be on the top surface of the generator. The generator selection is the 500W, 600rpm AC, 3 phase generator with an internal phase to phase resistance of 0.2ohms. The generator is mounted at the bottom plate of the top column with two sets of o-ring attached for water sealing purposes. The compression ratio of the O-ring is set to be 25 percent for both grooves. The floater column is sealed by welding rather than an O-ring design for better sealing and the connection between the floater column wall and the flange is welded with triangular aluminum blocks to reinforce the connection joint. The bottom tank is secured by two steel cones located on each side of the tank while the tank is filled with water. The wet mass of the tank is large in addition to the physical mass of the cones, it will provide sufficient mass to serve as the reactive body in the designed wave conditions.

During normal operation, the wave encounters the system and drives the buoy in a vertical direction. The buoy runs on the top column track via pre-installed wheels, which guide the buoy in a linear motion. The buoy is coupled with the push tube through the force sensor cage and the sensor measures the direct vertical force between the buoy and the second body system. The push tube is welded with an adapter that's bolted to the ball screw nut. The vertical oscillation on the push tube will back drive the ball screw and creates a bi-directional rotation. The ball screw is then coupled to the MMR and secured by two bearing mountings. The MMR is then converting the motion to the one-directional rotation and feed to the generator. The generator is a 3 phase generator so that 3 wires are soldered

to the extension wires and output from the very top of the system.

Sensors are also essential for the in-lab or open water testing. A load cell is located in the center of the cage and secured by seven bolts. Six-course bolts connected with the push tube located at the bottom, and one fine thread bolt connected to the top of the cage. The bottom side of the cage is only coupled with the top cage via three dowel pins with one side interference fitted, and the other side transitional fitted. During normal operation, since the ball screw is playing a major role in the powertrain, the buoy is likely to spin and cause unnecessary torque to the force sensor. Therefore, the dowel pins are designed to stop the torsion but permit relative motion between the two sides of the cages that allow the force sensor to detect.

The assembling of the WEC with the MMR PTO faces a lot of challenges. First of all, the majority of the system's powertrain is located at the top column, which significantly increases the center of gravity of the overall body. The center of buoyancy is mainly provided by the floater column in the center and the top column. Even with the tank filled with water, the center of buoyancy locates close to the center of gravity, which likely to cause the system's instability or even failure by the system not being able to stand up straight on the water surface. Second, the tank is designed to fill almost 3 metric tons of water, which creates huge force during the deployment phase on the structure. The bolts selection and connection tensile and shear strength have to be high in order to create a reasonable safety factor. Therefore, the size of the floater column needs to be carefully designed in order to have the system float on the surface of the ocean.

As shown in Figure 2.2, the hardware is prepared for the field test. With the newly designed large buoyancy column, the buoyancy center can be further increased so that the system can be more stable. With a detailed inspection, the O-ring design was not able to completely seal off the water so that another layer of O-ring on the bottom flange of the top column

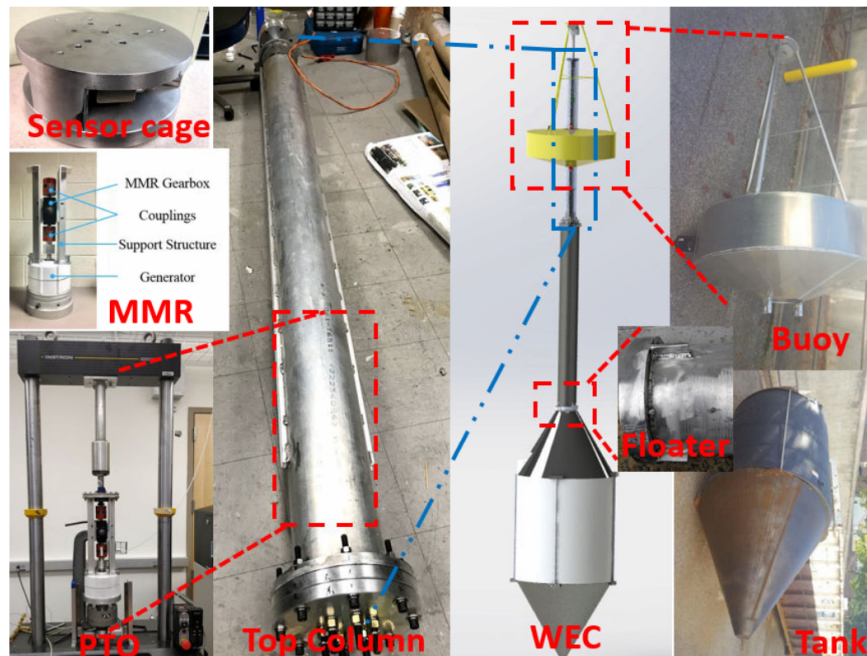


Figure 2.2: It shows the 1:20 scale 500W system hardware and CAD design. The system is MMR-based, which could help increase the overall efficiency of electric power generation. The tank is composed of two steel cones on each side of the plastic tank, and the two steel cones are connected by the aluminum round bars that are 1-inch in diameter. The final systematic testing has not yet been completed.

is added. Before the field test, an water sealing inspection will be completely thoroughly to prevent system's electrical component failure.

### 2.2.1 MMR Design and Power Transmission

As mentioned, an MMR system is designed to convert bi-directional rotation to unidirectional rotation. It is designed with two opposite side one-way clutches, six bearings and three shafts shown in Figure 2.3. Three bevel gears are also included in the system to redirect the power flow if needed. One thing to notice is that the both one-way clutches are located on the wave input shaft, and the output shaft is interference fitted with the bottom bevel gear with pins

going through, so the output shaft always rotate at the direction of the bottom bevel that it is coupled with.

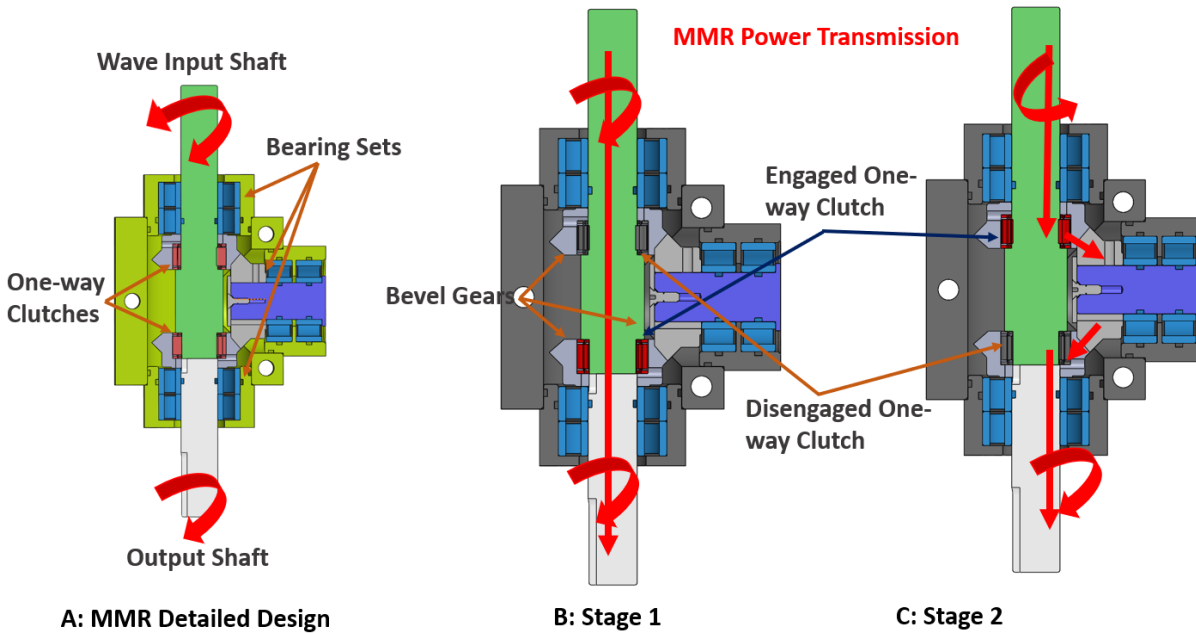


Figure 2.3: Mechanical Motion Rectifier design and power transmission figures. It shows both of the engagement modes.

In stage 1, While the wave input shaft is driven by the ball screw from the oscillating the buoy, observing from top of the MMR gearbox and assume the wave input shaft rotates clockwise, the top one-way clutch is disengaged so that no power flows to the top bevel gear from the wave input shaft. Therefore, the power keep flowing into the bottom one-way clutch. Since it is engaged, the bottom bevel gear located on top of the one-way clutch rotates as the same direction as the wave input shaft. Since the bottom shaft and the bottom bevel gear are locked together through welding, the power will directly flow through the bottom bevel gear from the wave input shaft, to the output shaft. The middle and top gears follows the motion. However, if considering the details of the top bevel gear rotation, it is obvious that the top bevel gear rotates at a different direction as the wave input shaft. However, due to the disengagement, the power will not interact between the top bevel gear and the

wave input shaft.

In stage 2, while the wave input shaft is rotating counterclockwise, by observe from the top, the top one-way clutch is engaged, and the power will follow from the wave input shaft to the top bevel gear directly. The top bevel gear drives the middle and bottom bevel gear directly. And due to the interference fit at the bottom, the output shaft will follow the rotation of the bevel gear and still rotate at clockwise direction. Since the stage 2 output shaft has a different rotational direction as its input shaft, the bottom one-way clutch disengages and allow the different motion to slip in between.

The MMR gearbox has two stages of motion with an extra disengaged working mode. While the generator damping is large and the output shaft rotates faster than the wave input, the output shaft will be disengaged so that the rotational speed is not forced to slow down to match with the input. This working mode of disengagement allows the MMR gearbox to maintain its energy level during a low input state.

### 2.2.2 Analysis on the MMR Dynamics

The systems with MMR and non-MMR were investigated and Figure 2.4 shows the PTO system's response for both MMR and non-MMR systems. The top figure shows the force on both of the systems. It comes to a trend that the force on the MMR tends to remain 0 around 5s, 10s, 15s when the input excitation motion is slowing down and has a negative acceleration, the kinetic energy stored in the equivalent mass will become the power source and start to power the generator, which makes it a self-powered subsystem that is decoupled from the input. Therefore, on the second figure, the MMR mechanism shaft disengages, before reaches 0, slowly decay and re-engages and pick up the speed. This mechanism could potentially reduce the power peak to average ratio. In addition, it can help the generator

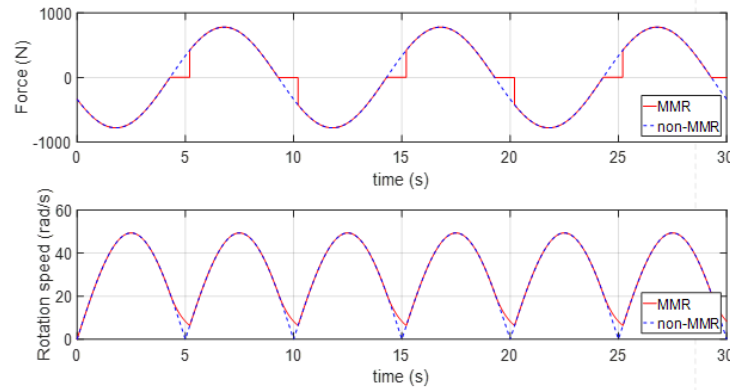


Figure 2.4: System's response for MMR and Non-MMR systems. The top figure shows the force on the system during the operation, and the bottom shows the rotational speed of the system with the disengaged at time of 5s, 10s, 15s, etc. [4]

to avoid the low efficiency zone at the very low speed, and improve the energy transmission efficiency.

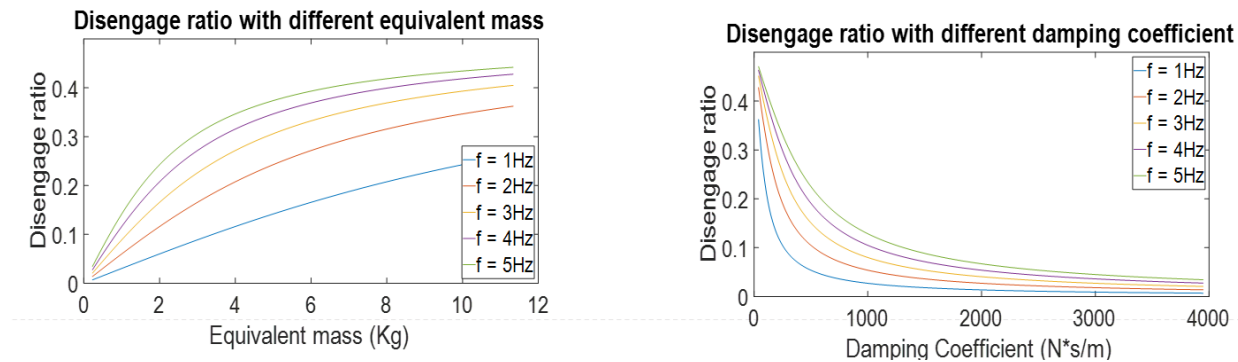


Figure 2.5: The system's force with respect to time under different resistive loads. [4]

To study the unique dynamic phenomenon of engagement and disengagement. The term disengage ratio is used here to present it quantitatively, the term represent the ratio of time the disengaged condition occupied in one period cycle. As shown in the figure2.5, the disengage ratio tends to increase while the equivalent mass increases. This is due to the large equivalent mass's rotation leads to more moment of inertia, so that after the system

will disengaged earlier, and reengaged later. As for the frequency lines, the higher frequency of engagement and disengagement will lead to a lower disengagement ratio due to the faster engagement speed.

As for the disengagement ratio compared to the damping coefficient, the trend is in the reverse direction. When the system contains a high damping, it will force the system to slow down faster passively to engage during the disengagement MMR gearbox. In the contrast to the figure on the left, the lower the frequency, the faster it is to reengage again in the MMR mechanism. The larger the disengagement ratio is, the power output should be higher compared with a traditional non-mmr system.

### 2.2.3 PTO Bench Test

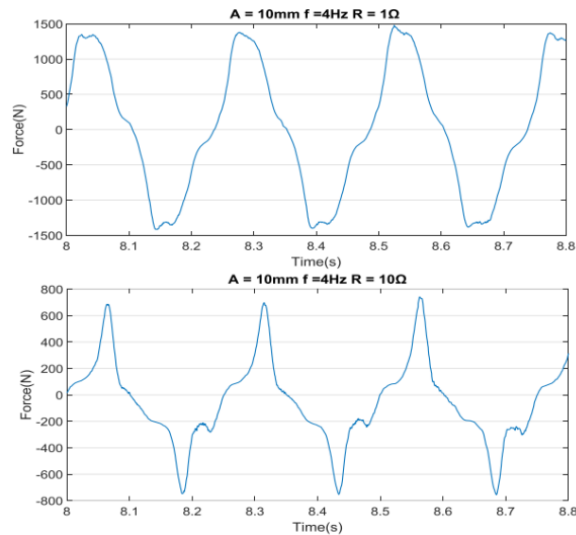


Figure 2.6: The system's force with respect to time under different resistive loads.[4]

The simplified PTO system was first built. The size of the bush tube and the ball screw were customized to fit the size of the Instron8801 stroke along with the adaptors. The PTO is coupled with the two surfaces of the Instron and driven by the hydraulic actuators to

simulate the wave. The figure shows the system force and response time under different external resistive loads. Figure 2.6 shows the force exerted on the PTO within a 10mm of displacement with a frequency of 4HZ. With resistance of 1 Ohm, the force could reach up to 1350N, whereas with the 10 Ohm of external resistance, the force is reduced to 700N. From the test result, it can be told that while the external resistance increases, the electric damping is smaller, and the disengaged period become larger, which matches the previous simulation result.

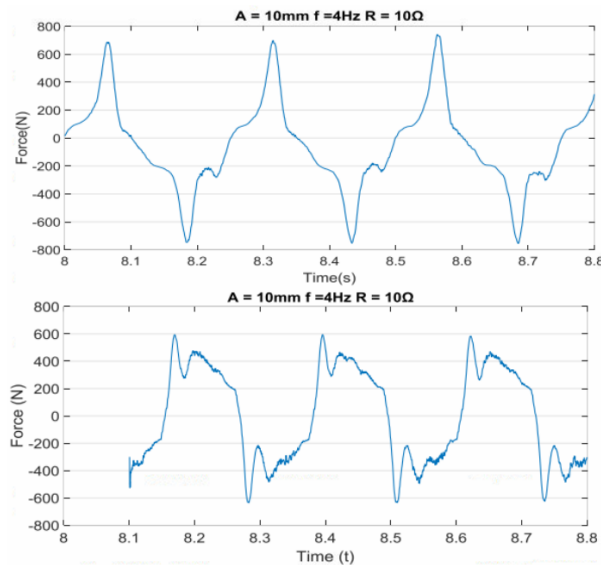


Figure 2.7: System's response with and without the MMR

Under the same excitation force, the system's behavior is different. From the above in figure 2.7, the two status of engagement and disengagement can be observed clearly. In addition, it can be noticed that the dominating force for the MMR system is friction when it is not engaged. For the non-MMR however, the form of the force input from the machine can be told to be the combination of the electric damping force from the generator and the friction [4]. Due to the existence of the backlash, some impact force can also be noticed.

The left figure shows that the system's efficiency vs. the linear velocity in the MMR and non

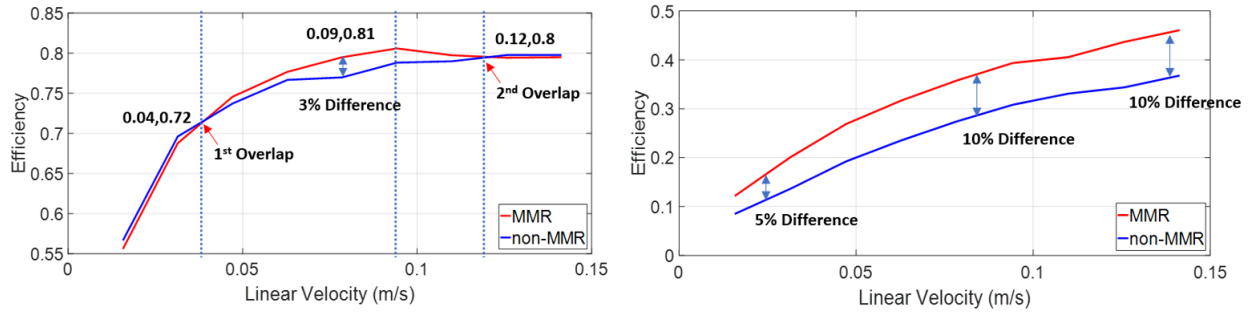


Figure 2.8: System's response and efficiency with and without the MMR[4].

MMR condition under the external resistance of  $1\Omega$  during the test. As the figure shows, the MMR based system has a relatively high operating efficiency which could reach even 81 percent. However, since the electric damping is larger, the disengagement ratio is small so that the difference between the MMR system and Non-MMR system is not obvious with the largest difference at 3 percent. The two overlap point represents the time that MMR performance decrease below the Non-MMR systems, while maintain similar at the same time.

While as the right figure shows that the external resistance is set at  $20\Omega$ , and the maximum difference can even reach 10 percent, which exceeded some previous designs. The reason for the difference is due to the larger external resistance lead to a smaller electric damping, which by referring to the previous figure, will increase the disengagement ratio of the MMR mechanism. Then lead to a higher MMR based system efficiency. With this test, it is clear that MMR has its advantage compared to the traditional direct drive system in the PTO under certain system damping. The system damping is affected by the adjustable electric damping, which can be adjusted via external resistance. Therefore, the external resistance has a huge affect on the system while aim at the optimum electric power output. This will be investigated further in Chapter 4 in the HWCEC device.

# Chapter 3

## Hybrid Energy Converter

The traditional marine energy point absorber is functional for energy harvesting for marine instruments powering, which suffers from low reliability from high PAR, and low power output. It is reasonable to predict that the power requirement for the marine energy converter to increase due to the higher demand on the marine applications. Therefore, wave energy harvester with solar panels on-board were then developed to mitigate the low wave energy input frequently. However, years of application shows the concerns of frequent environmental damage including wastes from animals and corrosion from sea water to the solar panel. To reduce the maintenance cost and increase the energy harvesting efficiency, a Hybrid Wave and Current Energy Converter (HWCEC) or short for Hybrid Energy Converter is developed, which brings a novel solution to the issues. It not only represents a new mechanism, but also a new way of thinking on the hybrid converters. The system can harvest energy from ocean wave and current simultaneously, and power the generator.

### 3.1 HWCEC Introduction

Researchers have been conducting investigation on the device that harvests energy from a single source such as ocean wave or current and the challenges are major: The single source energy harvesting could suffer from lack of energy input, which leads to low power output; Real ocean conditions introduce the irregular wave form that forces extreme PARs

to the mechanical system that could lead to low reliability and high maintenance cost, which directly contribute to a higher Levelized Cost of Energy (LCOE). This chapter introduces an combined mechanical system idea to relieve the mentioned issues, which harvests energy from both marine wave and current simultaneously. With the integration of power sources, prototype may achieve a much lower LCOE by producing more energy, while lowering the PAR with only a single PTO. However, without proper power transmission design, the system may under-perform due to the complex working modes and excessive back drives. Therefore, a hybrid gearbox is introduced in this study to joint the energy input sources, and output to the generator inspired from the previous gearbox designs [24] [25] [26]. The hybrid gearbox could combine the ocean wave and current input and unifies the output rotation for power generation at the same time. This combination also promotes the reduction of the electric power output PAR indicating a higher reliability, and promotes a low LCOE compared to a regular WEC device.

This chapter introduces a novel point absorber style PTO that implements the hybrid gearbox and harvests energy from both marine waves and current co-existing in the ocean. A dynamic model for the PTO is constructed focusing on the two-body WEC baseline along with the HWCEC modeling. The numerical results are then discussed and validated through the tank test and being compared after normalization. Despite the peak power promotion and the reliability improvement, the data is further analyzed on the generator's electrical damping and the PAR, and trends are discovered for these cases. It could help greatly with future control algorithm construction for marine energy harvesters in the future work.

## 3.2 Converter Design

The Hybrid Wave and Energy Converter is a combination of a regular WEC device and a hydro turbine design and harvests energy from both ocean Wave and current simultaneously. The detailed design and functionality of the hybrid gearbox system are introduced and showed a great advantage of adopting this mechanism. The turbine functionality and manufacturing process are then studied in order to provide the system more stability during normal operations.

### 3.2.1 Overall System Design

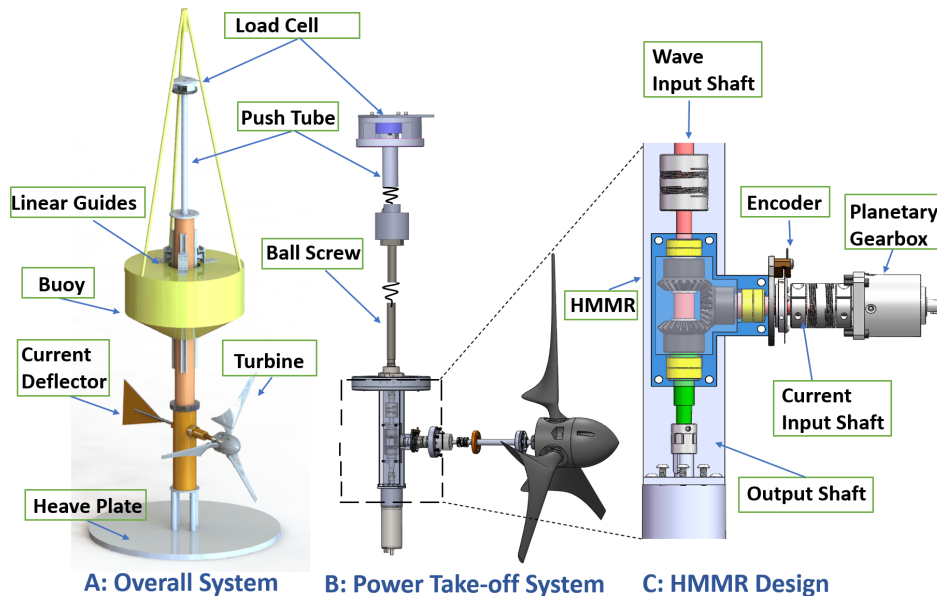


Figure 3.1: Overall system design. Figure A, B, and C shows the overall assembly, Power Take-off System, and Hybrid gearbox connection designs. The figure shows the general power flow and the design of the overall system.

The system consists of a two-body design that allows relative motion between the buoy and column with a heave plate as shown in Figure 3.1(A). This two-body design permit a wide

range of deployable locations since demand for supporting frame to the floating buoy during energy harvesting is required.

As the wave activates the system, the vertical motion of the buoy will be transferred to the push tube shown in 3.1(B). Then, the push tube lower end is bolted to the ball screw nut and transfer the motion to the ball screw. The back-driven ball screw mechanism converts bidirectional vertical motion to bidirectional rotational motion while being pushed vertically on the nut. The bi-directional rotation enters the hybrid gearbox from the wave input shaft.

On the current input side, as the ocean current reaches the system, the turbine starts to rotate unidirectionally. The turbine is coupled with a magnification planetary gearbox, which accelerates the current input speed to match with the wave input speed. With a coupled 3.5 magnification gearbox selected for this specific system, the rotation then enters the hybrid gearbox.

In Figure 3.1(C), the Hybrid gearbox's coupling with multiple input is shown. the function of the hybrid gearbox mechanism is to convert bi-directional rotation to uni-directional rotation and combines the wave input energy and current input energy to reach a higher power output level. The generator is directly coupled with the hybrid gearbox output shaft and produce electricity.

A current deflector is designed on the opposite side of the buoy to ensure that the turbine always face the current, and provide stabilization. At the very bottom of the system, the heave plate that has a large added-mass is attached to serve as the reactive body of the point absorber

### 3.2.2 Key Component Design

#### Hybrid Gearbox Design

The hybrid gearbox is the junction of the PTO, where collects the input energy from the wave and current, and output to the generator. The function of the hybrid gearbox is to convert bi-directional rotational motion to uni-directional motion and integrate input powers together. The hybrid gearbox contains bearings, bevel gears, one-way clutches, cases, and shafts listed in Figure 3.2.

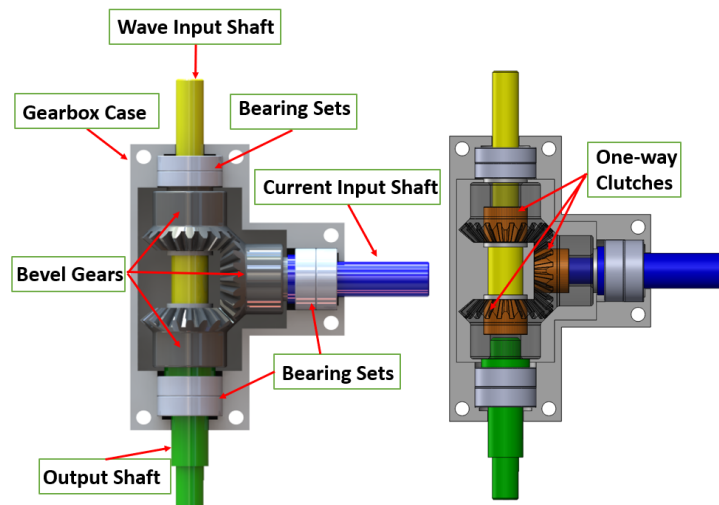


Figure 3.2: Section view of the hybrid gearbox design with a transparent view to display the one-way clutches. This figure shows the detailed component design of the gearbox.

Wave input shaft and output shaft are vertical with bevel gears' location shown in the figure. The wave input shaft has two one-way clutches installed and it is extended into the second bevel gear at the lower side. The lower bevel gear is locked with the output shaft so their movement are always stationary relatively. The horizontal shaft is the current input shaft, which also has an one-way clutch installed between the shaft and the bevel gear. All one-way clutches are located on the shafts, and inside the bevel gears. The function of the one-way

clutch is to isolate the motion between the inner shaft and the connected bevel gears and transmit only one direction of rotation due to the locking with the bevel gears. Furthermore, the shafts are well supported by the bearing sets and the gear meshing are well lubricated by grease.

The detailed power transmission design for working mode 1, wave input only is also shown in Figure 3.3. During normal operations, as one period of wave encounters the systems, the buoy moves vertically up and down and completes one period of energy harvesting. The gearbox wave input shaft is rotated in two directions sequentially from the back-drive ball screw's motion. Therefore, two stages of the power flow are established to perform the energy transfer, and each of them represents one direction of the wave input shaft.

In stage 1, the wave power is directly transferred from the wave input shaft to the output shaft without reaching the top bevel gear due to the disengaged top one way clutch. The bottom bevel gear and output shaft are driven by the wave input shaft with a engaged one-way clutch while the rest of the side bevel gears follow. From Stage 1, the top bevel gear rotates in a different direction comparing to the wave input shaft. Since a one-way clutch is located between the shaft and the bevel gear, it permits the contradictory motion.

In stage 2, the top one-way clutch on the wave input shaft is engaged so that the kinetic power on the wave input shaft will drive the top bevel gear, while other gears follow. As shown in Figure 3.3, the bottom bevel gear rotates in a different direction compared to the wave input shaft with the one-way clutch slipping in the middle. The bottom bevel gear directly drives the output shaft coupled with the generator.

The mode 2 condition represents the ocean current input only condition where ocean current input shaft is rotating faster than the wave input shaft and cause disengagement on the wave input side. Both wave input shaft one-way clutches are disengaged since the bevel gears are

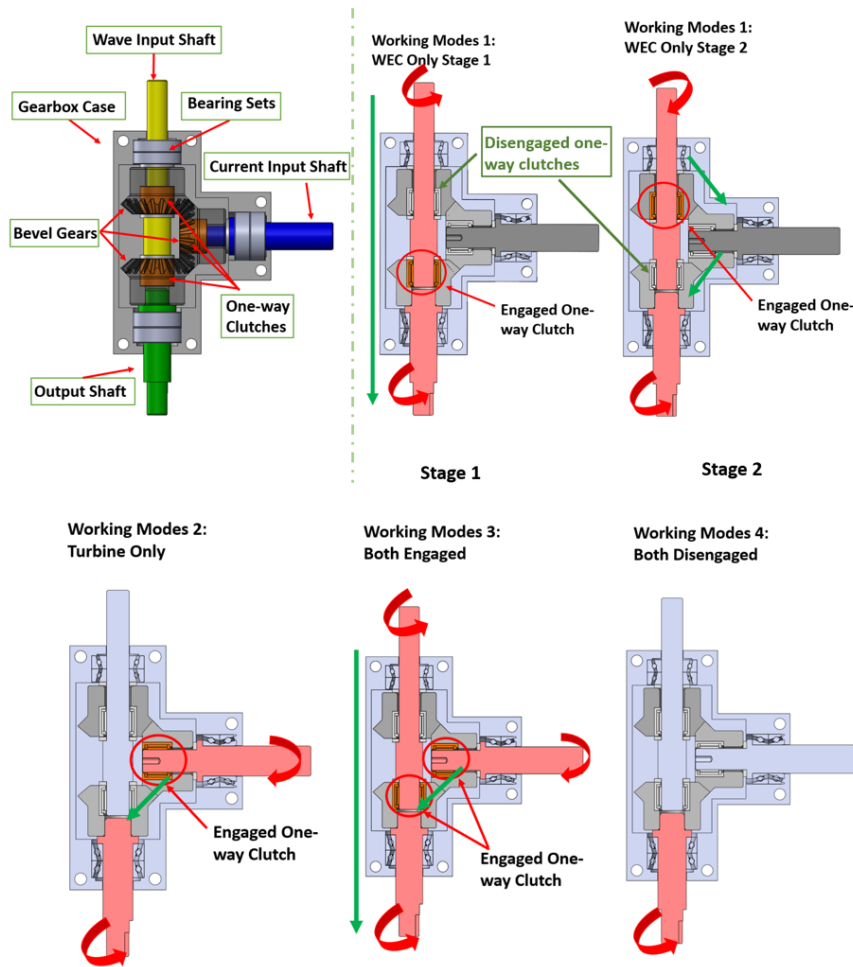


Figure 3.3: Hybrid gearbox design and designed wave only input power flow for mode 1. The mode is composed with 2 stages by the varying input rotational direction. Hybrid gearbox operation mode 2, current input only condition; Mode 3, wave and current both input engages, mode 4, no engagements

driven by the current input, and one of the one-way clutches is engaged via the different rotational direction while the other one-way clutch is disengaged via the slower wave input shaft speed. Mode 3 represents both shafts are contributing simultaneously to the output shaft when the rotational speed are the same. The occurrence of mode 3 is very limited due to the constant changing ocean wave input. Mode 4 shows that both shafts are disengaged while the inertia of the generator drives the output shaft faster than both of the input and

lead to triple disengaged one-way clutches.

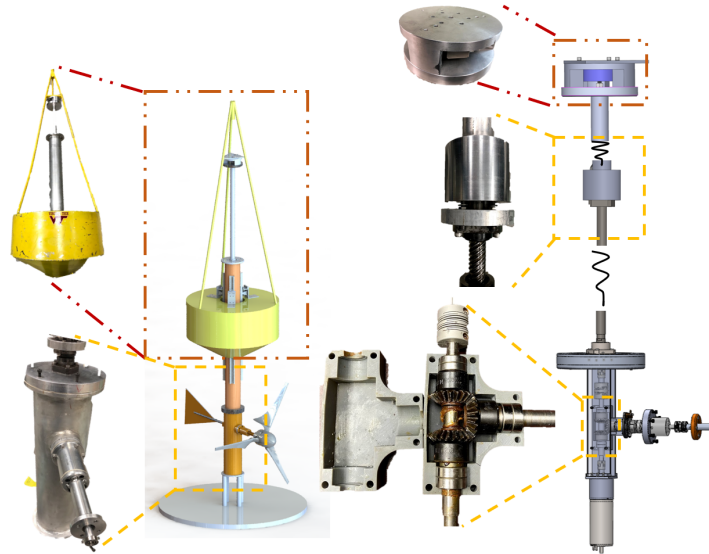


Figure 3.4: System hardware demonstration. It showed the general assembly of the HWCEC including the buoy, bottom column, ball screw connection, and Hybrid gearbox

Above all, the four working modes define the hybrid gearbox's function. Therefore, the hybrid gearbox is proved to be able to convert bidirectional rotation to unidirectional rotation shown in mode 1, and integrates the current input energy shown in mode 2, with high efficiency and robustness while selecting only the higher input. In special condition mode 3, both input could contribute simultaneously to the output, and in mode 4, where the PTO is conserving energy and disengage all input to prevent being forced to slow down and reduce energy output.

### Turbine Design

The turbine design is a commercialized turbine with a scaled-down process. This turbine is also designed to be used for current energy harvesting purposes [27][28]. In this work, we

have adjusted the size of the turbine in order to decrease the starting current speed/torque requirement.

In order to decrease the starting torque requirement, it is essential to decrease the overall weight of the turbine. The ultimate design is to manufacture the turbine's overall density to be similar to the water density, which in this case is close to  $1g/m^3$ . Therefore, selecting metal parts would not be an ideal choice due to the density limit. Hence, 3D printing technologies are used for this turbine manufacturing. During the preliminary test, our team selected Acrylonitrile Butadiene Styrene (ABS) to construct the surface and chose "Sparse" filling. ABS plastic's density is about  $1.1kg/m^2$ , and with the sparse filling, the turbine weight is well under  $1g/cm^3$ . XTC-3D coating has been chosen to be applied on the surface of the turbine to increase the surface smoothness and reduce friction. During the preliminary test, all of the turbine blades failed catastrophically at the root of the turbine due to the huge force applied from the current simultaneously. It is suspected that the regular wave-type also contributes to the failure of the turbine, where it might reach resonance with the incoming current and shatter the three turbine blades simultaneously. Furthermore, the turbine had trouble rotating from low input current speed due to misalignment, and waterproof design within the system.

Therefore, in the final tank test, Polyetherimide (ULTEM) as the turbine material is chosen, which has a much higher tensile strength and flexural modulus. Polyetherimide has a density of  $1.27g/m^3$ , and with the "Double Sparse" filling. Since the required turbine starting torque was high, the size of the blade was also increased to 20 inches in order to compensate for potential system frictions. XTC-3D coating was also applied on the surface of the new turbine to reduce friction and prevent water absorption. With the addition of some extra foam in the center of the turbine chamber, the overall turbine density is built to be close to  $1g/cm^2$ , and it doesn't have much tendency of floating or sinking in the water. However, the

turbine is found to be heavier than the water, and it has the tendency of sinking but very slow. It indicates that the bolts in the turbine might increase the overall density, but the weight will be balanced by the current deflector later to secure the overall system's stability.

The turbine blade angle can also be adjusted between tests for higher harvesting efficiency since blades were printed separately [29]. A planetary gearbox is directly connected with the turbine. It is coupled with the turbine shaft and the hybrid gearbox current input shaft. It is a commercial product that increases the rotation speed to 3.5 times higher, in order to match the range of the speed range of the wave input shaft. The planetary gearbox is also securely fastened on the case so that it can further reduce the misalignment. Circular gaskets are installed on the outer ring to prevent water leakage. An encoder is also installed on the shaft to count the shaft rotational speed after the planetary gearbox installation.

### **Water Sealing Design**

System robustness for the wave and current combined system is also very challenging due to the current harvesting methodology. Since the model contains a marine current input, the prototype requires liquid sealing designs on the ocean current input shaft. O-ring dynamic sealing has been adopted to prevent liquid from getting into the system. Large friction caused by the high compression ratio on the O-rings will cause the shaft to lose its energy harvesting efficiency. Low friction by low compression ratio on the O-rings will cause fast leakage to the system, which will corrode the metallic prototype and cause unnecessary damping in the generator. The water sealing method selection is extremely practical and challenging. Profound research on statics and dynamics water sealing have been conducted, [30]. However, not much dynamics sealing has been investigated on energy harvesting devices especially for a smaller scale prototype since friction is playing a significant role in the smaller scale devices.

To further reduce the operation friction and water leakage, the dynamic O-ring design for water leakage prevents needs to be redesigned. In the preliminary test, one O-ring groove was designed on the shaft with a compression ratio of 15 percent. The O-ring Compression Ratio is the division of the O-ring compressed distance over the original O-ring diameter. As a result, it not only jittered the system operation but also caused large friction on the shaft. Therefore, 2 O-ring grooves designs were selected after the preliminary test was done. The first groove that is closer to the turbine has a compression ratio of 7 percent, and the second groove has 10 percent. With these two grooves in place, it helped aligned the shaft position better, and also stopped the shaft jittering problem during operation compared to a rotary seal.

### 3.3 Dynamic Modeling

In this section, the HWCEC is investigated through the sub-system dynamic modeling that includes a wave energy converter, a marine current turbine, and a novel mechanical PTO to integrate the energy from both sources. The numerical simulation of the overall system performance is then performed by integrating the component-level model and the coefficients of a 1:10th scaled prototype. The scaled-down version better matches the tank test due to the restriction of the testing site. Therefore, a 1:10th scale scenario was chosen for better comparison.

### 3.3.1 Two-body WEC baseline

The dynamic modeling of the wave energy converter [31] is investigated in the heaving directions, which dominantly affects the power extraction:

$$m_1 \ddot{z}_1 = F_{e,1} + F_{r,1} + F_{d,1} + F_{k,1} - F_{pto} - F_f - F_{ks} \quad (3.1)$$

$$m_2 \ddot{z}_2 = F_{e,2} + F_{r,2} + F_{d,2} + F_{k,2} + F_{pto} + F_f + F_{ks} \quad (3.2)$$

where  $z_i, \dot{z}_i, \ddot{z}_i$  ( $i = 1, 2$ ) represents the two-body displacement, velocity and acceleration.  $F_{e,i}, F_{r,i}$ , and  $F_{k,i}$  ( $i=1,2$ ) are wave excitation forces, radiation forces, and hydro-static forces that could be calculated based on linear wave theory [31] with boundary element method.  $F_{d,i}$  ( $i=1,2$ ) stands for linearized viscous damping forces.  $F_{pto}$  stands for counteracting forces from PTO, whose detailed modeling could be found in [23].  $F_f$  stands for mechanical friction resulting from rails between the two bodies and is dominated by working loads.  $F_{ks} = k_s(\dot{z}_1 - \dot{z}_2)$ , stands for the forces from springs connecting buoy and submerged body, where  $k_s$  is the stiffness of springs.

### 3.3.2 Turbine Baseline

A Horizontal-axis turbine was used in the HWCEC for ocean current energy. In the scaled prototype, the turbine blade has 0.495m in radius and uses NACA 63621 as the cross-section. The dynamics regarding the ocean current energy can be modeled as

$$(J_t + n_p^2 J_c) \ddot{\theta}_t = T_t - n_p T_{gen} - T_f \quad (3.3)$$

with  $J_t$  being the rotational inertia of the turbine and  $J_c$  being the rotational inertia of the

shaft and the gearbox.  $n_p$  is the gear ratio of the gearbox that connects turbine and the PTO.  $T_{\text{gen}}$  stands for generator counteracting torque, and  $\ddot{\theta}_t$  is the turbine angular acceleration.  $T_t$  stands for fluid-induced torque on turbine and  $T_f$  stands for mechanical frictions.

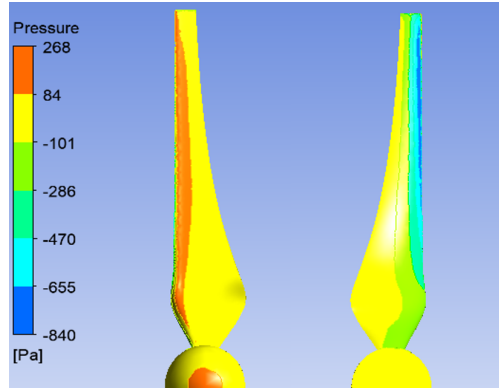


Figure 3.5: Marine Turbine pressure distribution on both front and back. The fluid velocity is 0.5m/s. The working condition is 15 RPM.

Figure 3.5 shows the pressure distribution on both sides of the turbine in a designed working condition. A pressure concentration can be seen around the leading edge, which brings potential risks of breaking. Therefore, the cord length around the root of the blade is further increased for robustness. The previous experiment suffered from turbine blade failure due to the force concentration. Better material with a higher fill rate was then selected to increase the robustness of the turbine blades.

### 3.3.3 Power Take-off

The HWCEC uses mechanical PTO to integrate the mechanical power from a point absorber and a marine current turbine and converts the mechanical power to electricity by driving a DC generator. In the PTO gearbox, two input shafts are respectively driven by the ball screw and turbine shaft. The output shaft connects a gearhead with ratio  $n$  and drives a DC generator. The counteracting torque of the generator  $T_{\text{gen}}$  is linear to the angular speed of

the output shaft  $\dot{\theta}_o$

$$T_{\text{gen}} = \frac{k_e k_t n^2 \dot{\theta}_o}{R_{in} + R_{ex}} \quad (3.4)$$

and the electric power is

$$P_{en} = \frac{k_e k_t n^2 \dot{\theta}_o^2}{R_{in} + R_{ex}} \quad (3.5)$$

where,  $R_{in}$  and  $R_{ex}$  represents the internal and external resistive loads from the generator's internal and external resistance, respectively,  $k_e$  is the electric coefficient, and  $k_t$  represents the torque coefficient.  $n$  is the gear ratio of the gear-head on the generator.

### 3.3.4 HWCEC Simulation Results

According to the environment and the energy flux between the ocean waves and ocean current, the HWCEC can have different working modes and have large variations in output energy. For the environment with sufficient energy flux in ocean currents and waves, the power performance of HWCEC is greatly increased and is better than the same WEC or turbine working individually. The output power of HWCEC, WEC, and the turbine are compared under different environments and working loads through numerical simulations. The time-averaged electric power is recorded. Details of working modes and system dynamics are referred to [32]. Numerical simulations are conducted for both WEC and HWCEC under regular waves with different wave heights while the wave periods remain the same at 2.21s.

The turbine power output simulated contour plot is shown in Figure 3.6. The turbine tends to have 7W of power under the current speed of 0.5m/s. During its peak power output, the

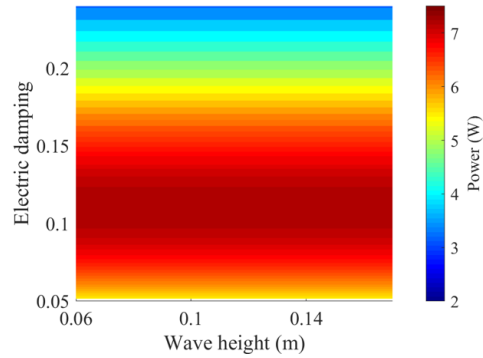


Figure 3.6: Output power for turbine baseline under different electric damping. The ambient flow velocity is 0.5m/s and the wave period is 2.21s

generator damping is close to 0.12Nms.

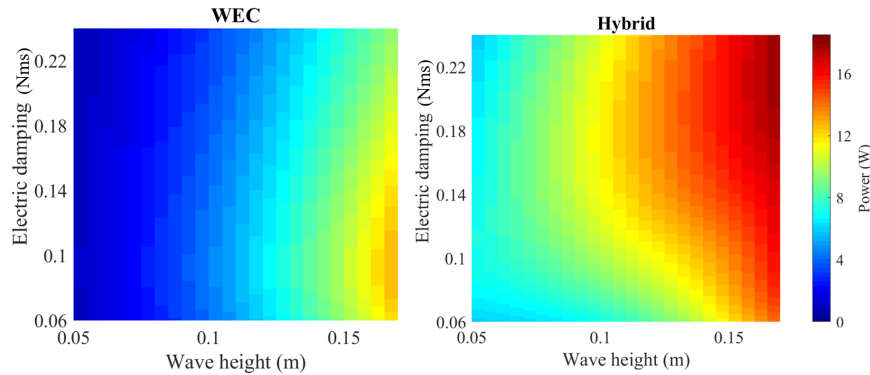


Figure 3.7: Comparison between WEC and HWCEC under different electric damping. The ambient flow velocity is 0.5m/s and the wave period is 2.21s

Contours are plotted for both WEC and HWCEC under regular waves with different wave heights while the wave periods remain the same at 2.21s. The undisturbed fluid velocity is 0.5m/s so that the turbine performance can be a baseline. The turbine power baseline is shown in Figure 3.6. The wave amplitude falls in the range of 0.05-0.17m. Similarly, the resistance is set in a range of 2.9-13.9 Ohm and the corresponding electric damping is from 0.24-0.06 Nm/s.

From Figure 3.7 the maximum power of HWCEC at 17.3W is higher than that of WEC under the same wave height at 11.9W. For the case studied, the WEC tends to reach the maximum power at around 0.093 Nms of electric damping while the HWCEC tends to reach the maximum power at a higher electric damping at 0.2Nms. In Table 3.1, the power at each different wave height is compared. The operational condition is also under the wave period of 2.21s with 0.5m/s of input current speed. The max power listed represents the highest power output of the given condition with the best matching electric damping.

Wave Height (m)	Max Power, WEC (W)	Max Power, HWCEC (W)
0.06	1.68	7.94
0.08	2.98	9.90
0.010	4.65	11.74
0.12	6.70	13.07
0.14	9.12	15.40
0.16	11.91	17.27

Table 3.1: The power of the system in different wave height in simulation

As shown in Table 3.1, as the wave height increases under the same fluid velocity, the maximum power is increasing for both WEC and HWCEC devices. Since wave height mainly contributes to the wave energy input of both WEC and HECEC devices, the less the wave height it is, the more advantage the HWCEC is showing. Therefore, in the certain application of the HWCEC device, the turbine is contributing much more than the buoy energy harvesting efficiency, which provides a significant advantage to this combination of designs.

As the case shown in Figure 3.8, the wave has 2.21s in period and 0.15m in height, and the current has 0.5m/s ambient velocity. The HWCEC can have including Turbine-engaged, WEC-engaged, and both-engaged working modes based on the angular speed of shafts in the PTO gearbox. The details of the working modes and the switching criteria could be found in [32]. The time-averaged power of the HWCEC in simulation is 13.2 W while that of the WEC and the marine current turbine are 9.9W and 7.0W. Comparing to WEC working in

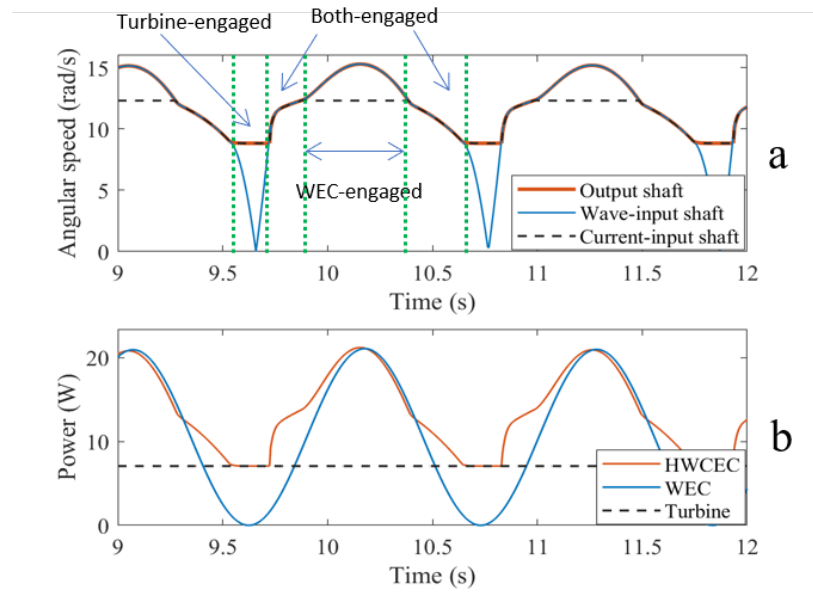


Figure 3.8: Time domain simulation on (a) rotational speed of the shaft under engagement and disengagement condition (b) HWCEC power output compared to WEC and Turbine only condition.

isolation, HWCEC has a power increment of 33 percent.

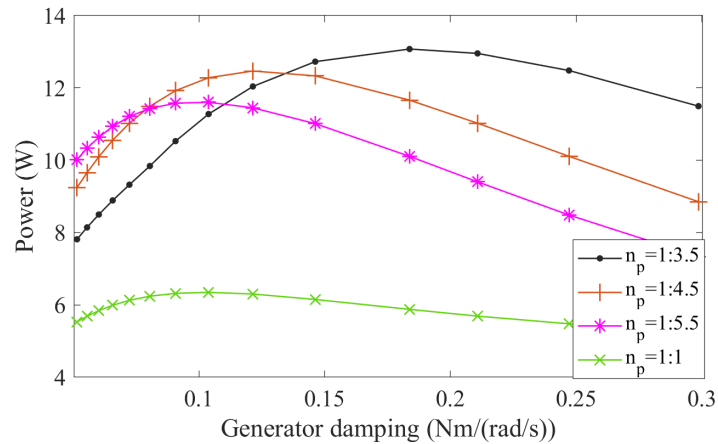


Figure 3.9: Effect of planetary gearbox ratio on the Hybrid device with related to the system's electrical damping. 1:3.5 gear ratio reached the peak in given conditions.

Numerical simulation is conducted on different settings of the gear ratio  $n_p$  between the

turbine and the PTO and the time-averaged power result is shown in Figure 3.9. For gear ratio 1:2.5, the HWCEC tends to require higher electric damping to reach the maximum power, which is impossible due to the relatively high inner resistive loads of the generator used in the tank test. As for the gearbox ratio of 1:4.5 and 1:5.5, both of the curves reached the peak power below the 1:3.5. Based on the power performance, the gear ratio 1:3.5 is selected for the planetary gearbox coupled with the turbine shaft for speed magnification.

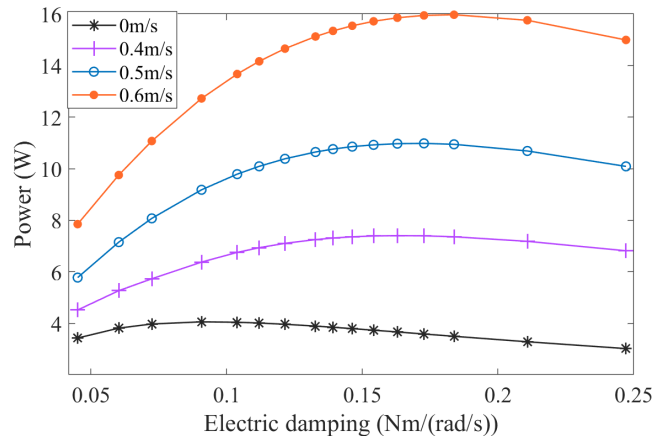


Figure 3.10: Varying speed input of the HWCEC with the amount of power generated under different electric damping. Wave height:0.096m, Wave period:2.21s.

Furthermore, the relationship between the power and load is also investigated to determine the best external resistance with regarding the hybrid system's best performance. According to Figure 3.10, while the current speed is increasing, the power output is increasing similar to comparing a WEC (0m/s current speed) device to a HWCEC. However, as the current speed is increasing with an increment of 0.1m/s, the increment of the electric damping corresponding to the max power is reducing, which tends to stay close to 0.17Nm/s in the given conditions. Therefore, this simulation results tends to indicate that for the 0.4m/s, 0.5m/s and 0.6m/s of testing data, the three peak output power corresponding electric damping may tend to remain close with each other and do not show significant difference.

# Chapter 4

## Basin Test and Discussion

Basin test is first introduced for the HWCEC system to verify the system's functionality. This chapter describes the testing plan of the system and analyzes the result. By comparing to a numerical simulation and test result, we can verify that the system does promote energy output under all wave situations. Both regular waves and irregular waves experiments have been performed. The advantage of implementing the hybrid gearbox and the turbine into the system is obvious. They do not only promote electric power output but also reduces the peak to the average ratio on the DCBL generator so that the system is more robust during the operation.

### 4.1 Basin Test

The preliminary test was conducted in the Steven Institute of Technology in New Jersey, USA, and the final test was conducted in the facility, Océanide, in La Seyne-Sur-Mer, France. The purpose of the preliminary test was to test the basic functionality of the system including power generation level, system stability during operation, and the identification of the measurement devices needed for the final testing. The entire process includes preparation, dry assembly, system inspection, system deployment, wet assembly, testing, and system retraction. Based on the facility infrastructure, our team worked with the facility managers to come up with a detailed system installation plan, mooring system, and test plan. All the

test results and pictures come from the final test that took place in Océanide.

### 4.1.1 System Preparation

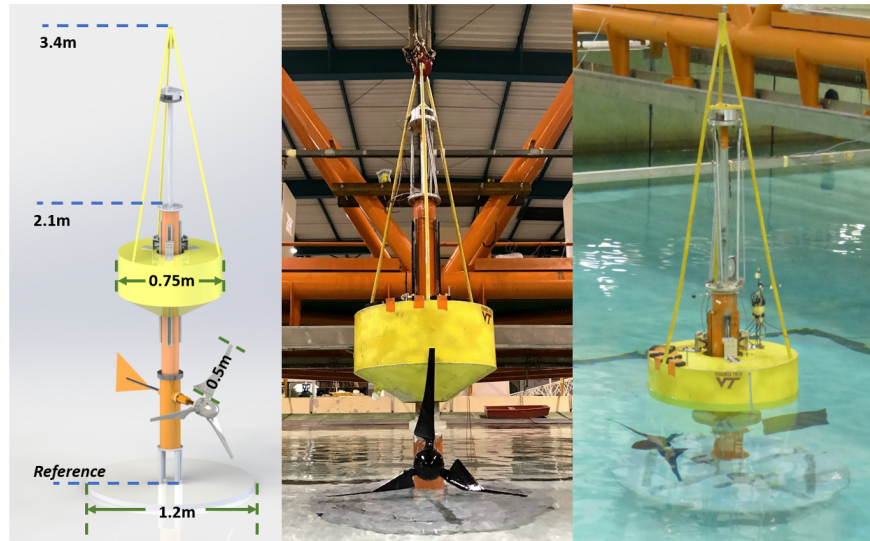


Figure 4.1: Dimensions, on-site assembly, trial testing. The current state of the system is extended.

The system was transported to Océanide in segments so that a dry assembly is first conducted before placing into the water. The PTO is expected to run smoothly with extra grease applied to the ball screw system. Basic system functionality was tested on a bench to confirm the optimum condition. After the power is measured via DAQ from the generator while the system is driven by hand onshore, the team can proceed with the column with PTO system assembly onshore.

After the dry assembly is completed, system balance is significant in the component level so that buoy and column need to be tested for balancing before the wet assembly. The buoy without the balancing tilts to the side, which will cause friction and obstruct normal PTO operations. The buoy condition is imbalanced due to the excessive salt stuck in the

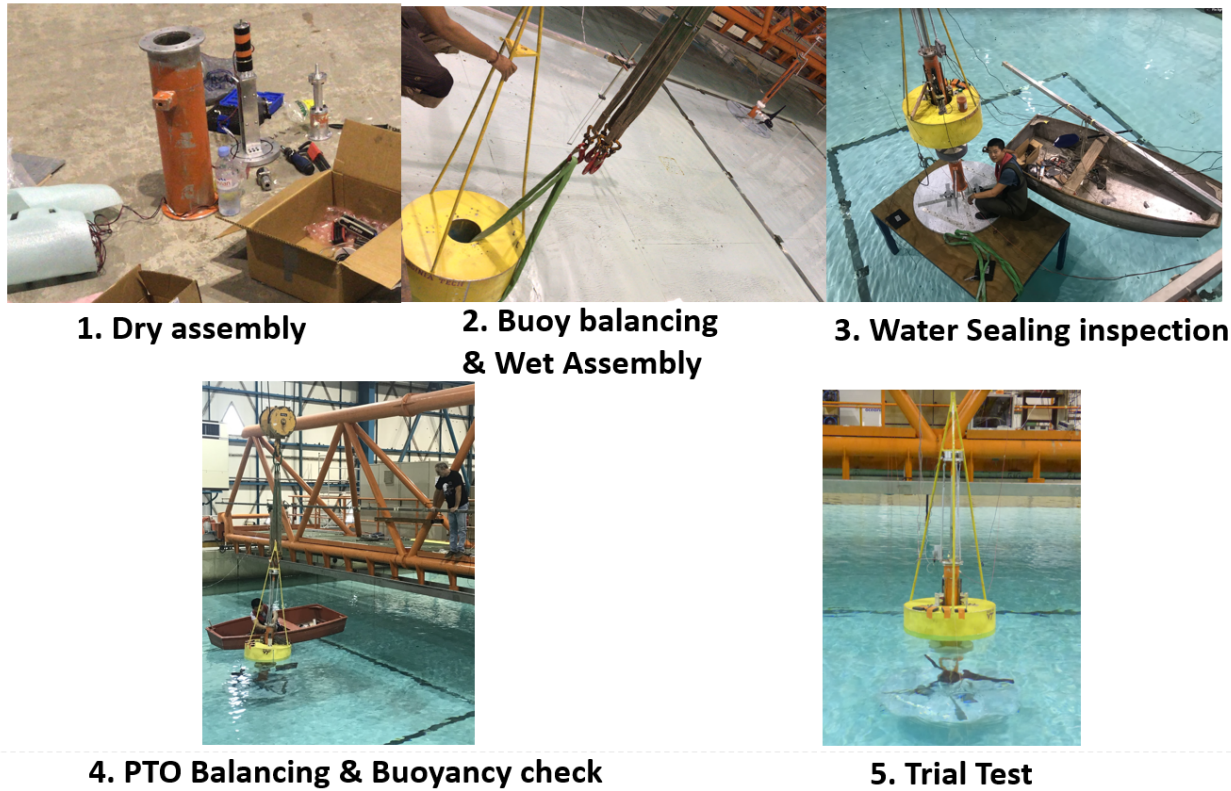


Figure 4.2: The basic concept of the system deployment for 5 basic steps

buoy bottom chamber from previous testings. Therefore, weight blocks were attached to the system for system balancing and it was checked by a digital level. Then the buoy was taken out of the water for wet assembly later.

Before the PTO column is sent into water, a throughout inspection for water leakage has been performed on the joints. Some of the gaskets was damaged during the transportation so that silicon glue was applied to the surface of the column to prevent water from getting into the system before the PTO enter the water.

The PTO column was then dropped to water for balancing. The horizontal balance of the second body is less complicated since the turbine material is slightly heavier than water, balanced out the current deflector located at the back. Vertical balancing is relatively chal-

lenging. The weight distribution and buoyancy require more adjustments. After calculation, a rigid circular foam was machined and tight around the column, which provides sufficient buoyancy and elevates the buoyancy center for the system's stability. In the meantime, the gravity center remains and the larger distance promises a more stable system. The PTO column was then taken out of the water and checked for potential water leakage or failure spot caused by the crane's lifting.

An overall system wet assembly compared to a dry assembly is extremely beneficial for this design. The dry assembly process will require the crane to lift up the entire system, which may cause unexpected damages to the system. On the other hand, a wet assembly requires all the segments dropped in the water first, and the technician uses cranes to assemble the overall system by segments. It greatly reduces the chance of damaging the turbine or the overall system since less weight will be carried by the crane.

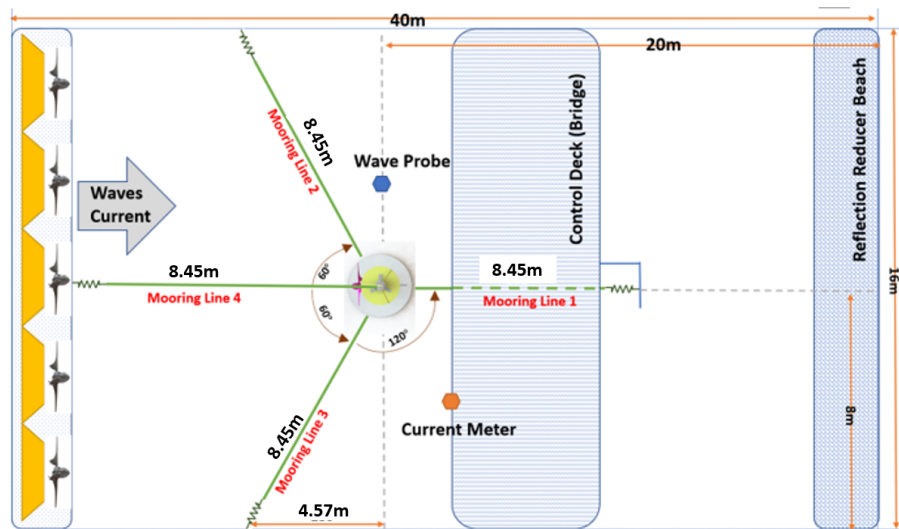


Figure 4.3: The overall layout of the testing facility. The Hybrid Energy converter is moored at the center of the tank while the turbine is always facing the current input direction.

The underwater platform in Océanide can be elevated so the deployment plan was to drop the PTO column into the tank on the platform first by using cranes, then drop the buoy onto the

PTO column with caution during the wet assembly process. Meanwhile, our team observes the buoy assembly with the PTO column. Very minimal space between the buoy center hole and the PTO column caused trouble and it requires an extra spotter to guide the dropping process under the buoy. The buoy is slowly dropped and when reaches the designated place as shown in Figure 4.3, our team tightened the buoy top triangular connector with the load cell housing.

After the buoy is connected with the sensor housing, the tank platform, and the crane drop simultaneously so that the relative position is kept the same. The platform and crane stop when the buoy can self-float on the water. When the buoy self-floats, the PTO column was still supposed to stand on the platform for later inspections. After the buoy was in place, guide wheels were then installed on the buoy and match with the linear guides on the column. Since the buoy was used multiple times in the previous tests, the surface of the buoy is not flat, which requires extra guide wheel balances. Washers are applied underneath the guide wheel adaptor on top of the buoy's flat surface to ensure the wheels are lined up. A slight angle between the wheel and the linear guide could potentially lock up the motion during the operations. The width of the guide on the PTO column is 0.25in wider than the wheel's thickness, which provides a misalignment solution. Grease is then applied on the track to prevent excessive friction between the wheels and tracks.

After the system is ready for the test after a detailed inspection, the test plan with reference tests and combined hybrid tests were laid out. As shown in Figure, the tank has a width of 16m and a length of 40m which is sufficient for our tests. However, in order to secure the data significance, we select data from only 150s to 450s. The wave and current were not able to reach a steady-state before 150s since it takes time for the wave and current maker to reach it's designed or designated speed. There will be a 10 minutes gap between tests for water to calm since the reflection wave may cause uncertainty even though a special platform

was built at the end of the tank, which reduces the wave and current reflection. The system is placed in the center of the tank so that the reflection wave on the sidewall be kept at its minimum.

The test plan was constructed so that it could completely fulfill the needs of this experiment. Our team has conducted the basic component tests such as the buoy only test and turbine only test by clamping either one of the input shafts. Since the system is built to isolate the two power sources so that no back-drive force will be consumed by the turbine while running the buoy only test, and vice versa. Then hybrid tests were then conducted include both turbine and buoy input energy. Three speeds of ocean current were tested: 0.4m/s, 0.5m/s, and 0.6m/s, and each of them corresponds to the wave period from 1.9m to 3m, wave height from 0.07m to 0.16m, and wavelength of 5.5m to 13m. Irregular waves were also mixed in for each ocean's current speed. For each test, external resistors of 4, 10, 20, 30, and 50ohms were used to determine the highest power efficiency. The designed testing condition may not be reached due to the calibration issue and data are analyzed case by case.

### 4.1.2 Mooring System Layout

While the system is operating on the water, mooring lines are usually needed to help stabilize the system and prevent the system from floating away due to the ocean waves and current. The mooring system is assembled with spring and mooring lines that are elastic and secured onshore so that it could maintain the system's location without locking it in place.

As shown in Figure 4.4, four mooring lines were used in the water tank to secure the structure, with three moorings installed on the heaving plate and another on the top of the second body. Through the pulley, the moorings remained parallel to the water surface to stabilize the HWCEC and restrict it from moving in surging and swaying directions while reducing the

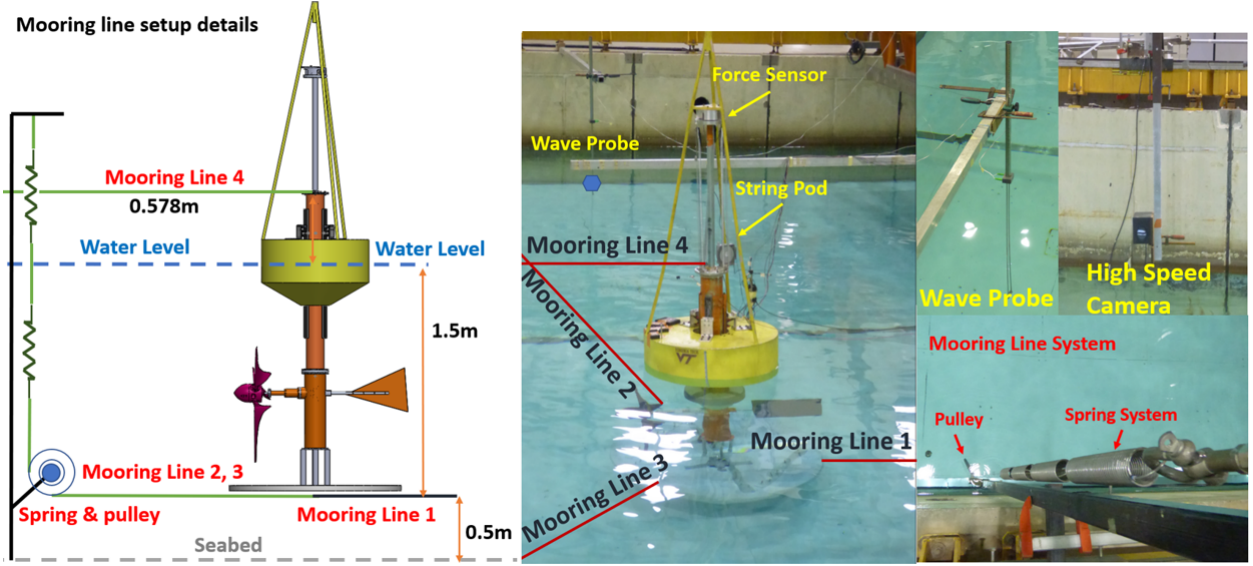


Figure 4.4: The detailed layout of the mooring constraint on the Converter. Four mooring lines are distributed across the overall system in order to secure its location and prevent large pitching motion from the wave and current.

effect on heaving directions. The end of the mooring lines connected to springs, whose stiffness is designed to avoid the resonance conditions in surge and increase the overall system's stability. The top mooring line (Line4) prevents the system from excessive pitching motion during the testing. All cables are connected with four spring systems with a pulley installed for guidance. The spring systems help provide the extra length during the testing when a large force is encountered. The system's natural period,  $T$ , in surge motion is calculated as:

$$T = 2\pi\sqrt{(m_1 + m_2 + A_{s,1}(\omega) + A_{s,2}(\omega)) / k_{m,e}} \quad (4.1)$$

$k_{m,e} = 3k_m$  where  $m_i$  are the masses of the buoy ( $i = 1$ ) and submerged body ( $i = 2$ ).  $A_{s,1}(\omega)$  and  $A_{s,2}(\omega)$  are the added mass of buoy and submerged plate in surging directions.  $k_{m,e}$  is the equivalent mooring stiffness in surge direction. For the mooring arrangement applied in the tank test shown in Figure 4.4. Based on a range of 1.5 s to 3 s wave periods in the tank tests,

$k_m$  was chosen to have a constant value of 150 N/m to avoid the resonance and improve the robustness of the tests. The corresponding stiffness is 15000 N/m for the utility-scale model based on Froude scaling. This brings simplicity in both deployment and modeling. In this sense, constant stiffness along the mooring line could be used as a reduced-order numerical model. Still, the elemental, high-fidelity models of mooring lines would be more accurate and would be meaningful for further detailed studies. The mooring force in the heaving direction is modeled as

$$F_m = -k_m n_m \gamma z_2 \quad (4.2)$$

where  $n_m$  is the number of mooring lines.  $\gamma = \frac{\sqrt{L_0^2 + z_2^2} - L_0}{\sqrt{L_0^2 + z_2^2}}$  is a non-dimensional number that represents the projection of the mooring forces in the heaving direction, with  $L_0$  being the mooring line's length. Because  $z_2$  is negligible when compared to  $L_0$ ,  $\gamma$  and  $F_m$  is close to zero.

### 4.1.3 Sensors Selection and Installation

Sensors are one of the most critical parts of recording data. Multiple sensors were installed on-board to measure force, motion, and power generations. Most sensors are attached outside the system except for the encoder, which measures the rotational speed of the turbine shaft. By reading the numbers off the chart, we are able to understand how the system functions during regular and irregular waves and help researchers foresee potential failure. Large motions on the buoy cause instability on the overall system and will destroy mooring lines so self-stability shall be maintained without the mooring system installed. With all the sensors in place, the experiment can finally start with data recorded onshore.

The location and the movement of the buoy are also essential to the test so that the motion sensors are installed on the side of the buoy to detect all direction movements. A total of six motions are in the scope: Pitching, yawing, rolling, surging, swaying, and heaving motion. Along with the mooring system design, the on-board sensors and in-water sensors are capable of getting the most accurate reading from the test. These data will contribute to the analysis of the buoy motion and system operating conditions. The load cell is also installed on the top of the system inside the adaptors. It measures the direct force between the PTO and the buoy. As mentioned previously, the load cell housing can eliminate all the torque but leave the only vertical force to the load cell for measurement. Together with the high speed camera, it is clearer to see how the relative motion between two bodies affects the system's power output and how force is related to the power generation. Furthermore, the encoder is attached to the wave input shaft on the hybrid gearbox inside the column in order to get the turbine rotational speed reading. The data transmission cable of the Encoder is bonded with the generator power output cable and exits from the top of the system to the DAQ onshore. After the sensors are installed, sensor initialization was performed so that the result is more accurate.

## 4.2 Results and Discussion

The tank tests have 3 phases in total. The HWCEC performance tests were conducted firstly with co-existing current and waves. The current remains 0.5m/s and the tested waves are shown in Table 4.1. The waves and currents are assumed to travel in the same direction. For each tested condition, a wide range of external resistive loads are tested for the tracking of the peak power.

The waves were scaled with a 1:10 ratio using Froude law from the model test in the DOE

Test	Wave Type	Wave Height [m]	Wave Period [s]	Wavelength [m]
1	Mono	0.048	1.57	3.83
2	Mono	0.063	1.79	5
3	Mono	0.07	1.9	5.63
4	Mono	0.096	2.21	7.65
5	Mono	0.125	2.53	9.99
6	Poly	0.0875	1.3	N/A
7	Poly	0.12	3.06	N/A

Table 4.1: Ocean environment parameters used in basin test

Wave Energy Prize. The irregular waves were set up based on JONSWAP spectra. Also, point absorber and marine current turbine were tested individually as baselines with the same condition shown in Table 4.1. During the test, a different gear ratio between the turbine and the PTO gearbox was applied for comparison.

### 4.2.1 Turbine Baseline Test

In the baselines that the turbine works individually, the flow velocity was 0.5m/s constant velocity. In addition to the external resistive loads, turbine performance is also tested with different gearbox settings to further tune the electric damping to track the maximum turbine output power.

The power performance of the turbine working individually with a 1:3.5 planetary gearbox is presented in Fig.4.5. The turbine reaches the peak power of 0.86W at 12 RPM at the generator damping of 0.06Nms. The power performance of the turbine working without a 1:3.5 planetary gearbox has a maximum power of 0.45W at 17.3 RPM at 0.15Nms. This result shows that the turbine's input power with the 3.5 magnification gearbox is significantly higher than that of the non-accelerated mechanism. It does match with the simulation result shown earlier that the 3.5 gearbox provides higher peak power, and none gearbox situation cannot reach the max due to the high internal resistance of the DC generator.

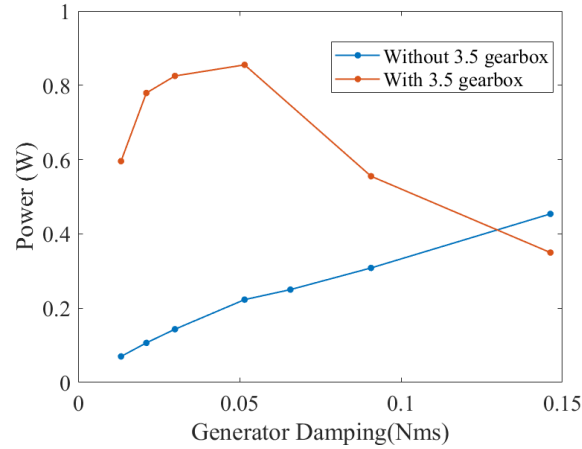


Figure 4.5: Turbine performance under different gearbox conditions with the change of generator dampings. The peak power is produced with the 3.5 magnification gearbox and reached 0.86W at a 0.5m/s current.

### 4.2.2 WEC Baseline Test

In the baselines that point absorber works individually, various external resistors with a range from 1 Ohm to 50 Ohm were applied to tune the electric damping, for each wave tested.

Table 4.2: Point absorber baseline tests result

Wave (Peak) Period [s]	Wave Height [m]	Max. Power, WEC [W]
1.57	0.058	1.12
1.79	0.093	1.928
1.9	0.076	0.92
2.21	0.102	2.78
2.53	0.143	3.76

The test wave conditions and results are presented in Table II. The wave height and the wave period are playing a significant role in the buoy baseline test. By increasing the wave period and the wave height, the power generated is generally increasing within the given condition.

### 4.2.3 HWCEC System Performance

For HWCEC, the system was tested with simultaneous ocean waves and current. The velocity of two inputs and one output shafts could indicate the working status of the PTO and thus provide information for the dynamic analysis. For the case shown in Figure 4.6, both marine wave and current provided energy input as the hybrid test. The current velocity is kept constant at 0.5 m/s and the regular wave targeted with the wave period of 2.21s, and wave height of 0.096 m. The external resistive load is 100Ohm.

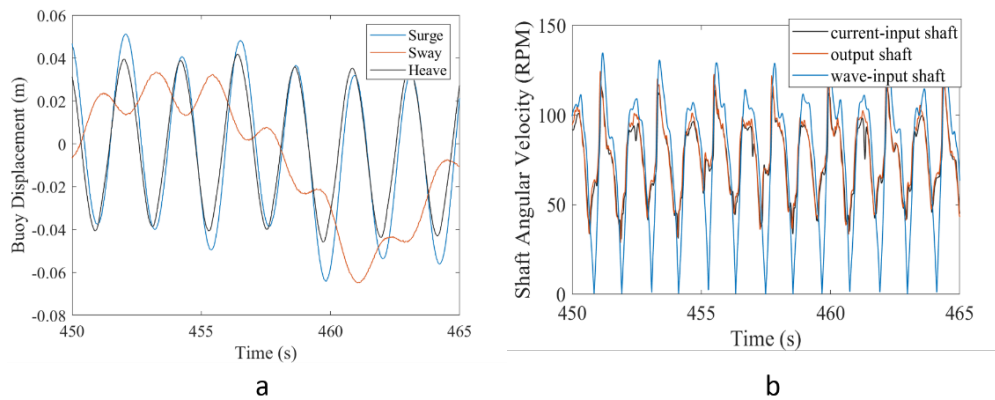


Figure 4.6: Experiment data recorded for a test under 0.5m/s current speed and 2.21s period regular wave. (a) Displacement of buoy (b) Angular velocity of input shafts and output shaft

As shown in the Figure 4.6 b, the graph shows the combination of the ocean wave input, current input and output shaft velocity. The current input shaft is experiencing an average of 0.5m/s of current input along with the system's self pitching. The wave input shaft indicates that the rotational speed dropping to 0 while the buoy is at its peak. However, the output shaft tends to follow the ocean current input while the wave input shaft speed is low, which is well-demonstrated in this figure.

The comparison of power output and shaft velocity is conducted between the Hybrid device and the WEC device working individually under the same loads. The result is shown in

Figure 4.7.

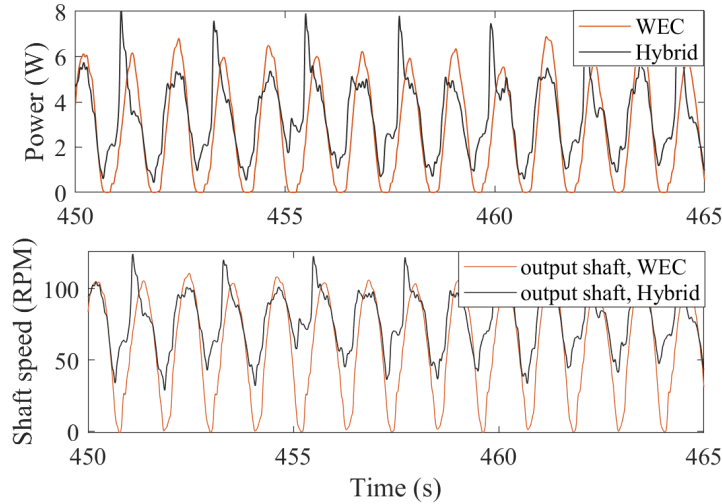


Figure 4.7: Comparison on power output and shaft velocity between the Hybrid device and the WEC device working individually under 10 Ohm loads and working environment.

In the figure, the WEC power output drops to zero during the motion. In contrast, the HWCEC output shaft will be driven by the current when the wave input is lower. Therefore, the velocity of the output shaft of the Hybrid system, which couples with a generator, will not drop to 0. This will increase of the electric power output and reduce the power output peak-to-average ratio.

As for the case studied, the WEC device has an average of 2.78W of electric power output. The HWCEC has an average of 3.15W of output. Due to the test calibration issue, the wave tested in the WEC baseline has a 0.102m wave height, which is 6 percent higher compared to the HWCEC wave height at 0.096m. Therefore, if synchronize the power put according to wave height, the normalized WEC power will be 2.46W.

In this case, with a constant external resistance set to  $10\Omega$  the hybrid device could promote the power from 2.46W to 3.15W with the turbine's implementation indicating a 28% increase.

However, this result does not represent the full advantage of a HWCEC since the external resistance could also bring variety into the power promotion.

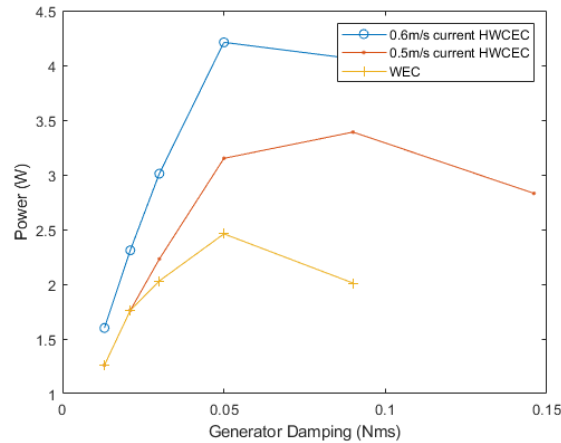


Figure 4.8: Comparison of the output power of WEC, 0.5m/s Hybrid and 0.6m/s Hybrid device with regard to the electric damping at the wave period of 2.21s and wave height of 0.096m.

The power performance of WEC and the HWCEC is tested under different generator damping to track the maximum power by switching the external resistors connected to the DC generator. As for the cases tested shown in Figure 4.8 with 0.5m/s of current, WEC has 2.46W of power output at 10 ohms of external resistance or with a 0.05Nms of generator damping. In the meantime, the HWCEC reached a maximum of 3.39W with 4 Ohm of load at 0.09Nms, indicating a 38 percent power increase under a regular wave condition. By increasing the current speed to 0.6m/s, the HWCEC has an increasing power from 2.46W to 4.21W, which indicates a 71 percent of power promotion.

The general data showed a increasing trend of generator damping from WEC to a 0.5m/s or 0.6m/s wave. However, due to the testing limitations, more data points between 0.05Nms to 0.1Nms were not discovered. Therefore, the optimal damping needs more future experimental data to discover the detailed trend.

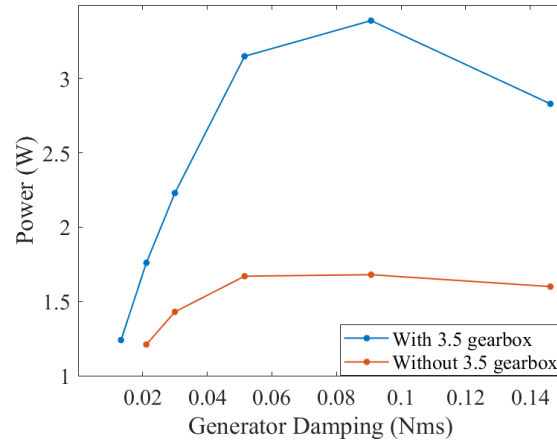


Figure 4.9: HWCEC power output with different gearbox configurations at 0.5m/s current speed. The Wave period is 2.21s and wave height is 0.096m.

According to Equation 3.4, the gear ratio between the energy harvesting structure has effects on the equivalent PTO counteracting torque. As for the Hybrid device, the ratio also has an effect on the working mode and thus is important to overall power efficiency. Comparison is conducted with different gearbox configurations between the turbine and the PTO gearbox and the result is shown in Figure 4.9. A 3.5 magnification gearbox between the turbine will increase the maximum power output from 1.68 W to 3.39 W, which is a 102 percent increment. This result indicates that during a scaled down test for the HWCEC, a gearbox is definitely showing its advantage of more than double the maximum power in this given condition. The peak without the gearbox reaches the peak at around 0.06Nms, while the HWCEC reaches the peak at around 0.09Nms of generator damping.

Figure 4.10 shows the experimental data of PTO power recorded in the irregular wave tests. As for the case studied, HWCEC has 2.92W time-averaged electrical power while the WEC, under the same condition, had 1.63W. That is 79 percent of electric power promotion in the irregular wave condition. Furthermore, the HWCEC had a lower peak-to-average ratio of the power output. In the case shown, the HWCEC has a peak-to-average value of 4, reduced

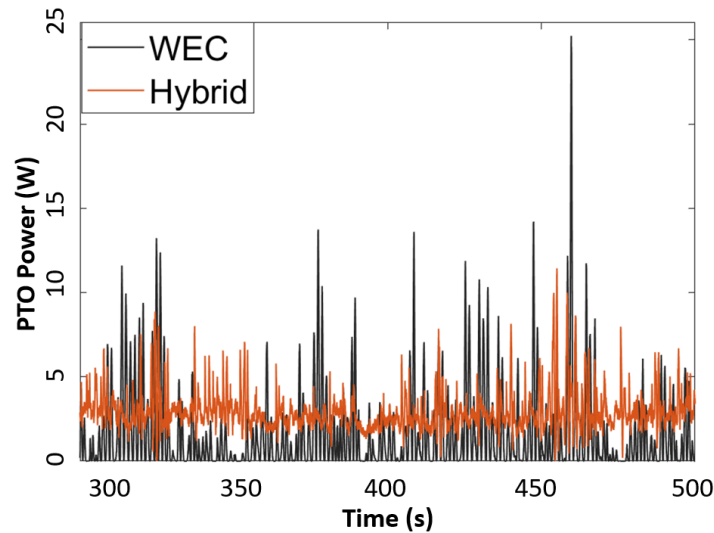


Figure 4.10: Comparison on output power between WEC and the Hybrid device under irregular waves with 3.06s significant wave periods and 0.12m wave height with 0.6m/s of current input speed.

from 15, which indicates a nearly 70 percent reduction.

In order to further investigate into the power output PAR, a detailed analysis for the irregular case mentioned above is shown in Figure 4.11. It is comparing the power PAR and the occurring percentage of the WEC and HWCEC.

As shown in the Figure 4.11, the PAR for HWCEC is reaching its maximum at 4, and the WEC is reaching the max at 15. The maximum occurrence percentage of the WEC is at 9 percent corresponding to 0.1 of PAR, which is lower than that of the HWCEC at 20 percent corresponding PAR at 1. However, the percentage for the WEC is slowly decaying while the PAR is increasing. It shows that the irregular wave condition forces the WEC system to harvest energy in all ranges of ocean conditions so that the occurrence percentage is relatively flat with slow decays. However the WEC does reach a high PAR of 10-15 in certain extreme cases, and the impulse of the large PAR could cause failure to the system. Lastly, the spreading out WEC PAR pattern produces less concentrated energy production,

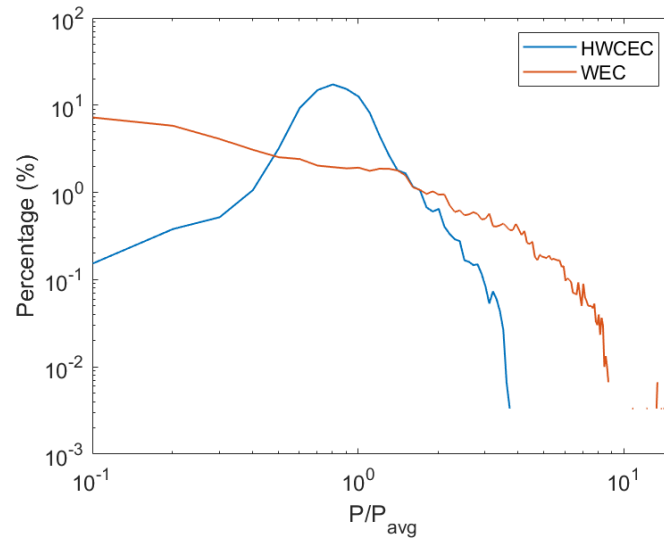


Figure 4.11: PAR and its occurrence for both WEC and HWCEC. The WEC device's ratio is more spread out in a decreasing pattern with the maximum at 15 while the HWCEC concentrates at the ratio of 1 with the maximum at 4.

and decrease the system's controlability in general.

On the other hand, the HWCEC tends to reduce the extreme PAR and performs an occurrence shape as the 2nd order polynomial, which peaks at the ratio of 1 at 20 percent, and quickly decays while apart from its center. It indicates the HWCEC operates at the PAR of 1, which is the exact average of the system's power output in the most possibility. The normal distribution of the HWCEC PAR exhibits its stability of power output during irregular wave condition, which could also introduces a predicable trend for further control algorithm construction. The significantly lowered ratio is also an indirect indicator of a more robust overall system design lead to a lower maintenance cost.

### 4.3 HWCEC Basin Test Conclusion

This chapter demonstrates a novel Hybrid Wave and Current Energy Converter (HWCEC) that simultaneously extracts energy from ocean waves and currents while using one single PTO through hybrid gearbox power integration. This configuration of design can bring HWCEC a power promotion of 38 to 71 percent in a regular wave condition and a 79 percent of promotion in irregular wave condition compared to a traditional MMR-based WEC. The system is proved at its optimum condition with the while the power output is increasing, the system requires a higher electrical damping to compensate the increasing power output. Moreover, the increasing electrical damping significantly decelerates when approach close to its optimum. According to the simulation and tank test result, the implementation of the 3.5 magnification gearbox and the external resistance at around 4 ohms which correspond to 0.07Nms of electrical damping will result in the highest power output.

A low PAR could reduce the load to the system, and it is an indirect indicator of a higher system's reliability and lower LCOE. The WEC device has a slow decaying and spreading out PAR with a maximum of 15 compared to a HWCEC's more concentrated pattern at 4, which indicates a 70 percent reduction. The more concentrated HWCEC PAR has a peak occurrence of 1 at 20 percent with a predictable pattern. This normal distributed pattern can be varied based on the combined system's design, which could be further analyzed for the future control algorithm implementation. The HWCEC's design, prototyping, simulation, and testing with analysis have been demonstrated in this paper. The novel concept has a high potential to be adopted for future ocean energy harvesters design, and marine instrument powering.

# Chapter 5

## Future Work on the Hybrid System

This chapter focuses on the variation of the Hybrid Wave Energy Converter design to fit the needs of the specific requirements, and future plans on improving the system stability and energy harvesting efficiency. The Hybrid system is recognized by many industrial partners for its high adaptability in the environment while maintaining high energy harvesting efficiency. The dual input design is capable of harvesting energy from marine waves and current simultaneously so that higher energy output in an individual device will result in less harvester weight that needs to be carried around. The requested weight limit is 50 lbs while the power output is at 300 W, which is a challenge for a traditional Wave Energy Converter. Therefore, the Hybrid system is further modified to meet the collaborators' requirements, and the Hybrid LITE system is introduced.

### 5.1 Hybrid LITE System Design

#### 5.1.1 Hybrid LITE PTO Design

The Hybrid Wave and Current Energy Converter was introduced in the past two chapters and the tank test proved its functionality and robustness. However, due to the requirement of the collaborators, the designs are usually modified to fit the needs. The Hybrid LITE system is a typical example of adaptive and modular design based on the regular HWCEC

but contains a completely new design language. Due to the requirement, the system has to be light weight, robust, and can be carried by two persons with sufficiency electric power output.

Therefore, in order to solve the problem, our team has introduced a new design of the Hybrid system that weighs less than 50 lbs to be fitted in a backpack. The system can be deployed or retrieved by a single person in less than 20 minutes. Once deployed into the ocean, the system can harvest an average of 300W power continuously on a 24/7 basis without maintenance. The system is modular and can be scaled up to provide more power if needed. The modular design also makes it possible to network with solar energy, wind energy, and diesel engine energy to provide comprehensive and reliable energy.

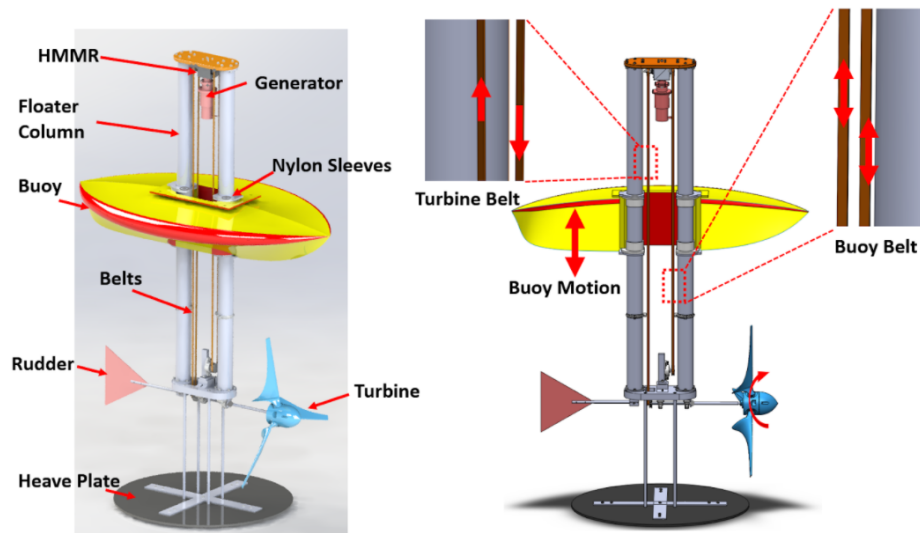


Figure 5.1: Overall Hybrid LITE system design

As illustrated in the last chapters, the proposed hybrid harvester consists of a wave energy converter (WEC) with a boat-shaped buoy, a submerged second body, a turbine for current energy scavenging, and a power take-off (PTO) system with a belt-pulley transmission. As the harvester is subjected to wave heave motion, the buoy oscillates up and down along

the guide column and therefore collects the ocean wave energy. The second body of the WEC is stabilized by a catenary mooring system. When subjected to ocean currents, the submerged turbine rotates and thus collects and transmits the ocean current energy to the PTO. To synergies the synchronous WEC and turbine motions, a hybrid transmission system is proposed in the PTO, as illustrated, based on the Hybrid LITE gearbox (HLG) gearbox which could convert the bi-directional wave-induced motion of a floating buoy into unidirectional rotation of an electrical generator. The bidirectional heave motion of the buoy and the rotation of the turbine are then regulated and transmitted to an electromagnetic generator at the top of the harvester through the belt-pulley transmission system. The powertrain is located above sea level so that it will not be infiltrated by water which would cause large friction or even malfunctions. The hybrid gearbox is capable of combining the synchronous motions of the WEC and turbine together and unifying the wave input shaft's bidirectional rotation to one direction rotation. Since the proposed hybrid energy converter could scavenge energy from both ocean waves and current with the hybrid gearbox for motion regulation, it has a significant improvement in power generation. The preliminary tank test results show that our previous hybrid gearbox-based hybrid energy harvester increases 38-70 percent in electric power output compared to the WEC or turbine working individually in regular waves. Such results demonstrate the potential of the hybrid energy converter as an efficient and cost-effective design [32].

In addition to high power output, the proposed harvester module will also be featured as ultra-lightweight, portable, package-able, and compact by elaborate material selection and elegant design. For example, the buoy will be designed to be inflatable and foldable. The harvester module can be folded and packed into a 37" luggage size backpack to be carried around, as illustrated in Figure, and the weights less than 50 lbs. The unfolding and setup process can be finished within 20 min by a single person. The device is also designed to

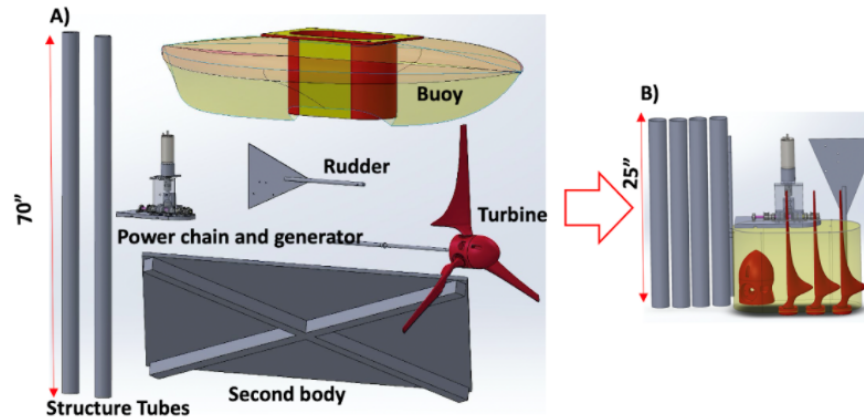


Figure 5.2: Compact design of the Hybrid LITE system to fit the needs of the clients

be retrieved quickly from the ocean with ease before moving to the next spot and thus reliable in-situ power supply on the go is guaranteed. The harvested energy is transferred to the power management circuits and stored in the battery bank on the shore to help generate electric power for the base. The system output is 12 V DC and 110 AC power and multiple systems are usually linked together for a larger power generation. Depending on the mission, the number of the Hybrid devices will be decided before each tour based on the ocean condition and the needs.

As shown in Figure 5.4, the left side is the turbine input shaft, which connects with the uni-directional rotating turbine facing the ocean current. The right side is the buoy input shaft, which is coupled with the oscillating buoy floating on the surface of the ocean. Therefore, the buoy input shaft on the HLG contains two directions of motion during operation. The power output shaft or the generator shaft is coupled to the generator located at the bottom of the gearbox. The entire connections are secured by O-ring placement so that they are completely water-tight. The angled assembly design is the best for the watertight and the O-ring groove is also placed in the center of the connection wall. The two input shafts both have an O-ring design to secure the structure's water tightness. Two sets of bolts on each

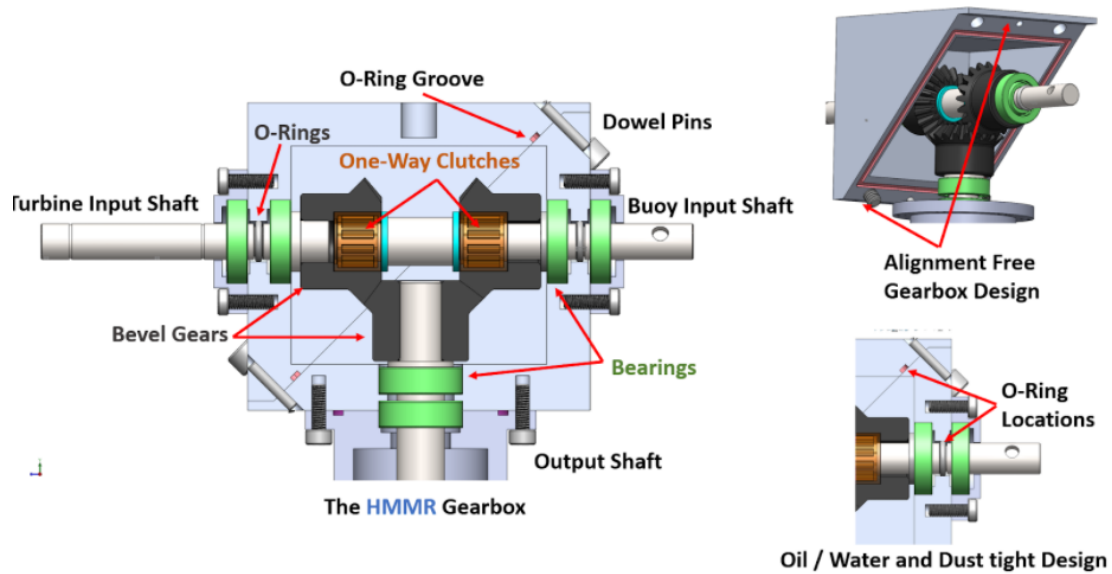


Figure 5.3: HLG cross-section view from the side. The figure illustrates the detailed design and components inside the HLG. The left figure shows the general structure of the HLG, which is similar to the hybrid gearbox described in the last chapters but with a different orientation. It helps the design in a narrower environment so that the system is more compact. The right two figures show the dowel pin alignment design to simplify the off-plane O-ring groove design.

wall are responsible for tightening the two sides of the gearbox so that the overall structure is stable.

### 5.1.2 Hybrid LITE Gearbox Design

Inside the gearbox, similar components compared to the hybrid gearbox are placed here. Two one-way clutches, three bevel gears, and six bearings are located inside the hybrid gearbox to support the power transmission and the structure. The thrust bearings are made from brass to prevent low mechanical efficiency due to excessive friction.

The gearbox case has a unique shape, which is manufactured by side-way milling on a slope.

The traditional design as the HWCEC hybrid gearbox case is separated into two halves through the middle as shown in Figure 3.3. However, from the basin test of the HWCEC, the gearbox experience misalignment issues on the bevel gears, which caused unexpected friction. The misalignment is caused by the center separation of the gearbox composition due to the placement of the bearings. The bearings' location are heavily affected by the contacting surface roughness and location, which is hard to control without a detailed carving process. Therefore, the side-way design is adopted so that the bearing slots are composed of full circle, rather than two half circles. This would eliminate or significantly reduce the misalignment from the design level. The other probable cause of the friction inside the gearbox is from the unsteady bearing support. Even though with the refined gearbox case for location accuracy, the bearing sets for each support are too close, which made the support performs as a point support. Therefore, in order to solve the continuous misalignment problem while under the strict space restrictions, bearings were placed as further apart as possible so that the supports from the bearings are acting as a surface supports. Bearings that locate on one shaft are then placed in both the inner and the outer side of the gearbox wall to generate better surface contact support.

Figure 5.4 shows the two directions of motion on the buoy input shaft, which is separated into two stages. For each stage, the rotational direction is defined based on looking at the HLG from the right side. For example, in stage 1, the buoy input shaft is rotating clockwise. The right one-way clutch is engaged, which is located between the bevel gears and the buoy input shaft. Therefore, the right bevel gear is also rotating clockwise. The middle bevel gear follows the motion of the right bevel gear. On the left side, the bevel gear follows the motion of the middle bevel gear and rotates counterclockwise. The turbine input shaft is pin press-fitted with the overlapping bevel gear so that all motion will be transferred from the gear to the shaft. The bevel gear is placed on top of the left one-way clutch and it

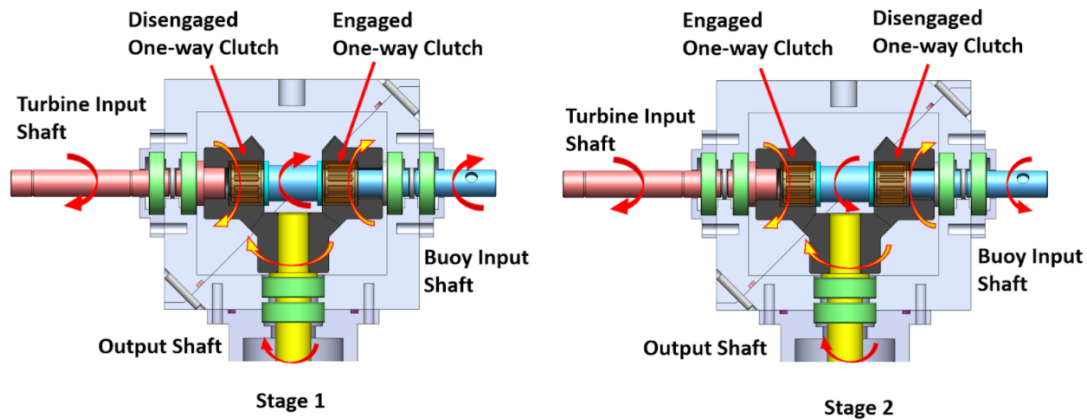


Figure 5.4: The power transmission of the HLG. The turbine input shaft, buoy input shaft, and output shaft are shown in red, blue, and yellow. Two stages of the HLG are shown so that the power transfer direction can be better seen.

is not engaged. Therefore, the different motions between the turbine input shaft and the buoy input shaft are not contradicting themselves. While the turbine input shaft is sent in rotational motion from the input shaft, it is coupled with the power from the buoy input side and combines them to the output shaft to rotate the generator unidirectionally.

In stage 2, while the buoy is going towards another direction in the oscillating motion, the buoy input shaft is rotating counterclockwise. The right way-clutch is then disengaged and the left clutch is engaged. Therefore, the motion from the buoy input shaft is not coupled to the right bevel gear located on top of it. Instead, the motion from the buoy input shaft is transferred to the left bevel gear since the left one-way clutch is engaged. It will then turn the left bevel gear counterclockwise as well. Then the turbine input shaft is turning counterclockwise as well. The middle bevel gear is then driven by the left bevel gear and rotates, followed by the right bevel gear. At this moment, the right bevel gear is rotating in a different direction compared to the buoy input shaft. However, since the right one-way clutch is disengaged, the motion is decoupled and it will not cause friction. In this case, even though

the buoy input shaft is turning in a different direction compared to its motion at stage 1, the output shaft rotation direction consists. Therefore, the HLG is capable of transferring the bi-directional rotation to uni-directional rotation despite the oscillating condition of the floating buoy. Furthermore, if the buoy input rotates faster, which will directly drive the turbine input shaft and consume energy. Therefore, another one-way clutch is designed outside of the HLG system located inside the pulleys on the left side. Therefore, it could prevent the back-driven condition and promise the most efficiency. This concludes the working mode 1 for the HLG.

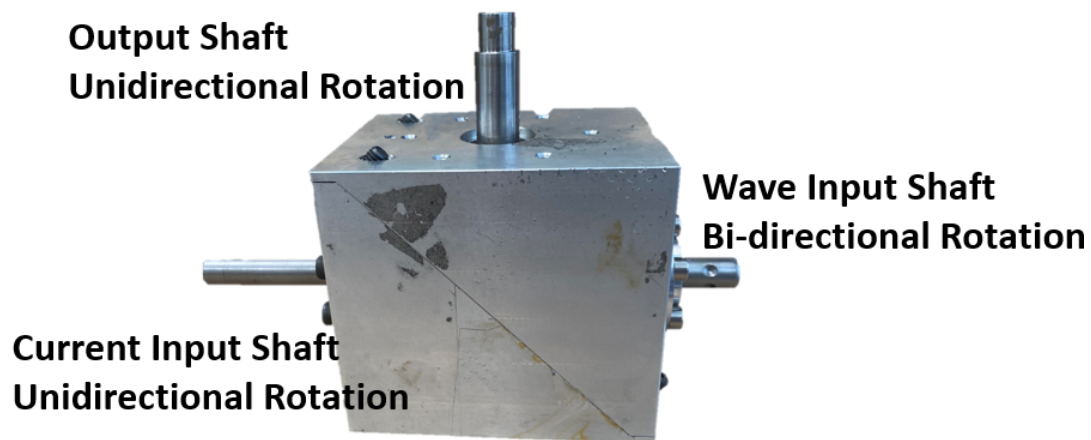


Figure 5.5: Customized Hybrid LITE Gearbox hardware. It is designed for open water applications with high reliability. Gearbox is ready for next phase hardware testing.

Similarly to the HWCEC, the HLG also contains four working modes and mode 2 is when turbine is the only input, while it is driving faster than the wave input shaft. Mode 3 explains that both input sources have the same rotational speed, which contribute equally to the generator. Last but not least, mode 4 represents the disengagement of the input from the output since output is rotating faster than both of the input shaft. These working modes will be investigated further in the future study in the hydrodynamics analysis of the overall

system.

In 300W power range, small-scale permanent magnet generators and brushless DC motor (BLDC motor) are the available choices. Permanent magnet AC generators are usually large and heavy because of their larger internal coil, in contrast, the BLDC motors are smaller and lighter due to fewer coil wraps but with a higher rotational speed. According to the requirement of the overall system's center of gravity, the generator module which is located at the top of the device needs to be less than 3kg. Thus, the BLDC motors are the better choice over the permanent magnet generator, and by considering the motor's weight, the power generated under working condition, heat loss, and rated rotational speed, a 220w DC brushless motor and a planetary gearhead with a gear ratio of 15.51 from NanoTech were chosen to be used as a generator module. From the data, the shaft rotational speed could reach up to 220rpm, and can be magnified to roughly 3400rpm for the DCBL.

## 5.2 Future Work Summary

Hybrid LITE converter is introduced in this chapter, which focuses on the modification of a existing HWCEC to a custom made to size multi-sources harvester. This design concept change motivated the study into system's reliability and potential challenges. Even though the design of the Hybrid LITE has been completed, with the potentially reduced PAR, control algorithm can be implemented to assist the system to operate smarter for a higher energy output and increase the life-span. The turbine design was adopted from a commercialized product[27] [28], and it is believed that a customized turbine shall be designed for the Hybrid LITE so that maximum power output can be obtained.

# Chapter 6

## Conclusion

Ocean is a huge source of energy and ocean wave/current energy harvesting has a great potential. In this thesis, the MMR-based wave energy converter and a hybrid energy converter are investigated. The MMR-based wave energy converter takes advantage of novel transmission mechanism to make the electrical generator rotate in one direction instead of rotating back and forth with the wave oscillation. The Hybrid energy converter harvests both ocean wave and ocean current power with one device. Design, prototype, and testing of both devices are done, with conclusions as follows:

1. The MMR-based energy converter is able to increase the conversion efficiency by 10%;
2. The hybrid energy harvester is capable to harvest both ocean wave energy and ocean current with one PTO with a novel mechanism hybrid gearbox designed to joint the energy combination;
3. The hybrid energy harvester is able to harvest 38 percent of extra energy from ocean current in regular wave conditions. Then, irregular wave model was selected and the power promotion can get up to 79 percent.
4. The PAR, especially during the irregular wave condition, is reduced by 70 percent, which is an indirect indicator of a better reliability.
5. The application of the turbine to the HWCEC not only reduce the PAR, but also much more gathered and peaks at PAR of 1. Which indicates that the peak power occurrence is at its average most frequently.

6. Probability decreases while PAR derives from its peak, and form a curve concave downward. This significantly increases the predictability of the PAR trend, and it is fundamental to the future control algorithm construction.
7. Identify the trend for the electrical damping of the maximum power output at between 0.05 and 0.09Nms for the proposed HWCEC. Especially when current input is added to the system, the resistance value tends to converge at a certain value. However, since the number of data point are not sufficient so that only estimated polynomial is provided. Further testings shall be conducted with regard to this trend in order to identify the actual relationship between the system and the external load.
8. Introduce Hybrid LITE for real life applications integrating seawater immersive design,requires few to none maintenance. It can also generator 200W of power while can be fold into a backpack. This system

Hybrid Energy Converter is a concept that merges wave and current energy harvesters, and forms a higher performance and reliable harvester at a lower cost. This thesis covers the combination of a wave energy converter and a marine turbine harvester according to the reference models. Along with the optimization on the design and PTO, it is also possible to create other types of joint system that would be even more efficient in energy production contribute to the journey of powering the blue economy in the short future.

# Bibliography

- [1] G. Lubineau, P. Ladevèze, Construction of a micromechanics-based intralaminar meso-model, and illustrations in abaqus/standard, *Computational Materials Science* 43 (1) (2008) 137–145.
- [2] C. Liang, J. Ai, L. Zuo, Design, fabrication, simulation and testing of an ocean wave energy converter with mechanical motion rectifier, *Ocean Engineering* 136 (2017) 190–200.
- [3] X. Li, C. Liang, C.-A. Chen, Q. Xiong, R. G. Parker, L. Zuo, Optimum power analysis of a self-reactive wave energy point absorber with mechanically-driven power take-offs, *Energy* 195 (2020) 116927.
- [4] X. Li, Design, analysis and testing of a self-reactive wave energy point absorber with mechanical power take-off, Ph.D. thesis, Virginia Tech (2020).
- [5] G. E. S. Yearbook, *World energy statistics* (2019).
- [6] B. E. Layton, A comparison of energy densities of prevalent energy sources in units of joules per cubic meter, *International Journal of Green Energy* 5 (6) (2008) 438–455.
- [7] I. E. Agency, [Ocean Power](https://www.iea.org/reports/ocean-power) *iea paris* (2020).  
URL <https://www.iea.org/reports/ocean-power>
- [8] K. Budal, J. Falnes, Wave power conversion by point absorbers: A norwegian project, *International Journal of Ambient Energy* 3 (2) (1982) 59–67.
- [9] K. M. Crosset, *Population trends along the coastal United States: 1980-2008*, Government Printing Office, 2005.

- [10] A. E. Copping, R. Green, R. J. Cavagnaro, D. S. Jenne, D. Greene, J. J. Martinez, Y. Yang, [Powering the blue economy - ocean observing use cases report](https://doi.org/10.2172/1700536)[doi:10.2172/1700536](https://doi.org/10.2172/1700536).  
URL <https://www.osti.gov/biblio/1700536>
- [11] A. Clément, P. McCullen, A. Falcão, A. Fiorentino, F. Gardner, K. Hammarlund, G. Lemonis, T. Lewis, K. Nielsen, S. Petroncini, et al., Wave energy in europe: current status and perspectives, *Renewable and sustainable energy reviews* 6 (5) (2002) 405–431.
- [12] V. S. Neary, B. Gunawan, C. Michelen, A. A. Fontaine, P. Bachant, M. Wosnik, B. Straka, R. Meyer, Us department of energy (doe) national lab activities in marine hydrokinetics: Scaled model testing of doe reference turbines., Tech. rep., Sandia National Lab.(SNL-NM), Albuquerque, NM (United States) (2013).
- [13] K. Budar, J. Falnes, A resonant point absorber of ocean-wave power, *Nature* 256 (5517) (1975) 478–479.
- [14] F. d. O. Antonio, Wave energy utilization: A review of the technologies, *Renewable and sustainable energy reviews* 14 (3) (2010) 899–918.
- [15] A. F. Falcão, J. C. Henriques, L. M. Gato, R. P. Gomes, Air turbine choice and optimization for floating oscillating-water-column wave energy converter, *Ocean engineering* 75 (2014) 148–156.
- [16] A. de O Falcão, Control of an oscillating-water-column wave power plant for maximum energy production, *Applied Ocean Research* 24 (2) (2002) 73–82.
- [17] D. Elwood, S. C. Yim, J. Prudell, C. Stillinger, A. Von Jouanne, T. Brekken, A. Brown, R. Paasch, Design, construction, and ocean testing of a taut-moored dual-body wave

- energy converter with a linear generator power take-off, *Renewable Energy* 35 (2) (2010) 348–354.
- [18] M. French, R. Bracewell, Heaving point absorbers reacting against an internal mass, in: *Hydrodynamics of Ocean Wave-Energy Utilization*, Springer, 1986, pp. 247–255.
- [19] D. Pizer, C. Retzler, R. Yemm, The opd pelamis: experimental and numerical results from the hydrodynamic work program, in: *Proceedings of the EWTEC 2000 European Wave Energy Conference*, Aalborg, Denmark, 2000, pp. 227–234.
- [20] S. Salter, Progress on edinburgh ducks, in: *Hydrodynamics of Ocean Wave-Energy Utilization*, Springer, 1986, pp. 35–50.
- [21] A. Bahaj, L. E. Myers, Fundamentals applicable to the utilisation of marine current turbines for energy production, *Renewable energy* 28 (14) (2003) 2205–2211.
- [22] S. Dajani, M. Shehadeh, K. Saqr, A. Elbatran, N. Hart, A. Soliman, D. Cheshire, Numerical study for a marine current turbine blade performance under varying angle of attack, *Energy Procedia* 119 (2017) 898–909.
- [23] X. Li, C. Chen, Q. Li, L. Xu, C. Liang, K. Ngo, R. G. Parker, L. Zuo, A compact mechanical power take-off for wave energy converters: Design, analysis, and test verification, *Applied Energy* 278 (2020) 115459.
- [24] X. Li, D. Martin, C. Liang, C. Chen, R. G. Parker, L. Zuo, Characterization and verification of a two-body wave energy converter with a novel power take-off, *Renewable Energy* 163 (2021) 910–920.
- [25] D. Martin, X. Li, C.-A. Chen, K. Thiagarajan, K. Ngo, R. Parker, L. Zuo, Numerical analysis and wave tank validation on the optimal design of a two-body wave energy converter, *Renewable Energy* 145 (2020) 632–641.

- [26] Y. Liu, L. Xu, L. Zuo, Design, modeling, lab, and field tests of a mechanical-motion-rectifier-based energy harvester using a ball-screw mechanism, *IEEE/ASME Transactions on mechatronics* 22 (5) (2017) 1933–1943.
- [27] B.-F. Chen, L.-C. Chen, C.-c. Huang, Z. Jiang, J.-Y. Liu, S.-y. Lu, S.-S. Leu, W.-m. Tien, D.-m. Tsai, S. Wu, The deployment of the first tidal energy capture system in taiwan, *Ocean Engineering* 155 (2018) 261–277.
- [28] H.-n. Wu, L.-j. Chen, M.-h. Yu, W.-y. Li, B.-f. Chen, On design and performance prediction of the horizontal-axis water turbine, *Ocean Engineering* 50 (2012) 23–30.
- [29] B. Jiang, X. Li, S. Chen, Q. Xiong, B.-f. Chen, R. G. Parker, L. Zuo, Dynamics of a hybrid wave-current energy converter with a novel power take-off mechanism, in: *Active and Passive Smart Structures and Integrated Systems XIII*, Vol. 10967, International Society for Optics and Photonics, 2019, p. 109670U.
- [30] P. Seals, *Parker o-ring handbook (ord 5700)*, Parker Seal Group, Lexington, KY (1992).
- [31] J. Falnes, A. Kurniawan, *Ocean waves and oscillating systems: linear interactions including wave-energy extraction*, Vol. 8, Cambridge university press, 2020.
- [32] B. Jiang, X. Li, S. Chen, Q. Xiong, B.-f. Chen, R. G. Parker, L. Zuo, Performance analysis and tank test validation of a hybrid ocean wave-current energy converter with a single power takeoff, *Energy Conversion and Management* 224 (2020) 113268.